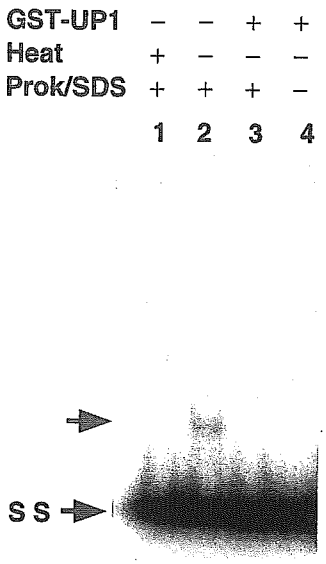

Figure 3 An electrophoretic mobility shift assay of CGG7 and UP1. A gel shows the formation of a bimolecular secondary structure from oligonucleotide CGG7 and the unwinding of the structure by UP1. Concentration of CGG7 was 20 nM and 10 nM, respectively. Concentrations of GST-UP1 were 0 μM (lanes 1, 2), and 3.7 μM (lanes 3, 4). Lane 1 was a heat-denatured control at 95 °C for 3 min just before electrophoresis. The sample mixtures were treated with proteinase K before electrophoresis, except for those in lane 4.

at much closer sites to the 3′ end of the primer than bacterial DNA polymerases (Fig. 4C). Addition of GST-UP1 reduced the arrest of DNA synthesis (Fig. 4C lane 3) and the same amount of GST had no effect on the arrest of DNA synthesis (Fig. 4C lane 2).

Next, we examined the effect of UP1 on the CD spectrum of CGG16 under conditions similar to that for the primer extension reaction. The primer-annealed template was first incubated in the presence of 150 mM KCl at 37 °C for 3 h and diluted ten-fold with the reaction mixture (final 15 mM KCl). After the same treatment as described previously, the CD pattern of oligonucleotide CGG16 in the presence of 15 mM KCl was similar to that observed in the presence of 150 mM KCl, namely a weak positive CD band at 280 nm and a strong negative CD band at 255 nm (Fig. 4D). The positive peak at 280 nm was increased by the addition of GST-UP1 dose-dependently (Fig. 4D), suggesting that UP-1 unfolded the non-B structure of the CGG16 to a certain extent under the same potassium ion concentration used in the primer extension reaction.

Kinetic analysis of the interaction between UP1 and d(CGG) repeats

Because stable binding of UP1 to the oligonucleotides CGG7 and CGG16 was hardly detected by electrophoretic mobility shift assay (see Fig. 3 lane 4), we performed kinetic analysis of the interaction between UP1 and d(CGG) repeats using a surface plasmon resonance (SPR) biosensor, BIACORE system. By monitoring the real-time interaction between GST-UP1 and $d(CGG)_{10}$ repeats with the BIACORE system, the association of UP1 with $d(CGG)_{10}$ was revealed to be rather fast, although the dissociation was still faster (Table 1). Although the affinity of GST-UP1 to $d(CGG)_{10}$ was 80-fold lower than that to $d(GGCAG)_8$, it is nevertheless rather high (see K_D values in Table 1). The affinity at 15 mM NaCl rose 40-fold compared with that at 150 mM NaCl. The K_D values of GST to $d(CGG)_{10}$ were more than 1000-fold higher than that of GST-UP1 (data not shown), and the affinity of GST-UP1 to $d(CGG)_{10}$ can be therefore equally estimated as that of UP1 without the GST-tag.

Table 1 Kinetic parameters for interactions between GST-UP1 and $d(CGG)_{10}$

Oligonucleotide (NaCl)	Association rate constant k_a (M^{-1} s^{-1})	Dissociation rate constant k_d (s^{-1})	Equilibrium dissociation constant K_D (M)
$d(CGG)_{10}$ (150 mM)	1×10^5	4×10^{-2}	4×10^{-7}
$d(CGG)_{10}$ (15 mM)	4×10^5	4×10^{-3}	1×10^{-8}
$d(GGCAG)_8$ (150 mM)	2×10^4*	1×10^{-4}*	5×10^{-9}*
pRandom40 (150 mM)	5×10^3*	2×10^{-3}*	4×10^{-7}*

These parameters were calculated from both associating and dissociating curves with an SPR-based biosensor. 'NaCl' indicates the concentration of NaCl in a buffer used for monitoring each interaction. *Parameters obtained in our previous study (Fukuda *et al.* 2002). pRandom40 is a random 40-mer oligonucleotide sequence and contains ten of each four nucleotides (Fukuda *et al.* 2002).

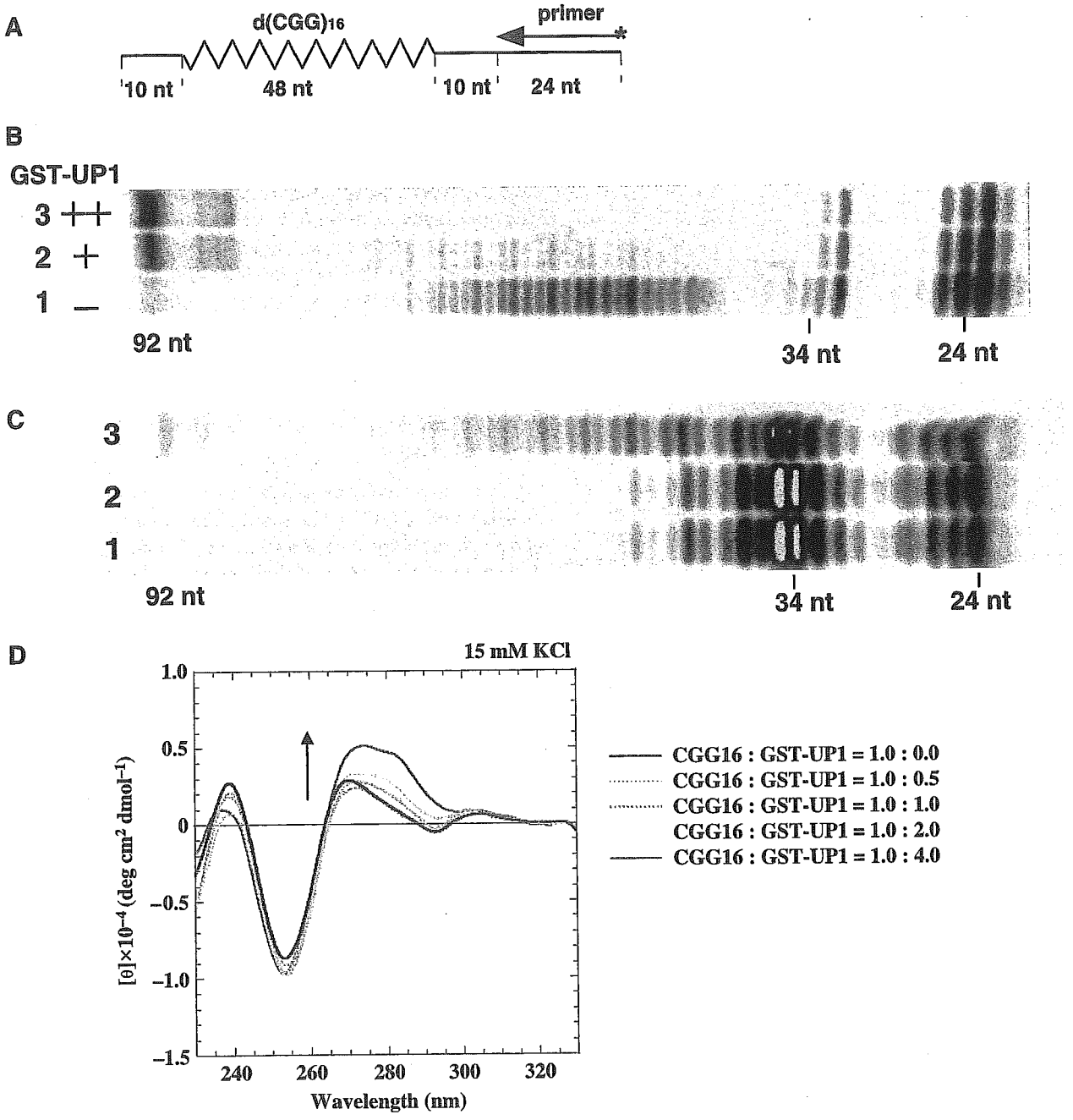

Figure 4 Effect of UP1 on the arrest of DNA synthesis at d(CGG) repeats. (A) Schematic representation of oligonucleotides used for the primer extension is depicted. The synthetic oligonucleotides, pM13-20 of 24 mer and pSubCG16 of 92 mer carrying $d(CGG)_{16}$, were used as primer and template, respectively. The zigzag line indicates $d(CGG)_{16}$ repeat on pSubCGG16. (B) Results of the primer extension reaction of *Bca*BEST DNA polymerase with or without GST-UP1, using the pSubCGG16 (final 10 nM) as a template. The concentrations of GST-UP1 were 0 M (lane 1), 125 nM (lane 2), and 750 nM (lane 3), respectively. The sizes of the fragments are indicated in nucleotides (nt) under the panel. (C) Results of the primer extension reaction of DNA polymerase α using the pSubCGG16 as a template without other proteins (lane 1), with GST (lane 2), and with GST-UP1 (lane 3). The concentrations of both GST and GST-UP1 were 3 μM. Grey portions in the bands of 34 and 35 nt show the areas over-exposed, in other words, beyond linearity. (D) CD spectra of CGG16 titrated with GST-UP1 in the presence of 15 mM KCl. From each spectrum, the spectrum of the corresponding protein is subtracted. Arrows indicate the changes of positive peaks of CD spectra as the concentration of the added GST-UP1 increased.

Discussion

The expansion of the d(CGG) repeat in the *FMR1* gene leading to the onset of Fragile X syndrome could be caused by formation of unusual DNA structures within the repeat during DNA replication. There are many reports analyzing the secondary higher structure of the repeat *in vitro* using various methods including CD, NMR, electron microscopy, and DMS-methylation analysis. The conclusions of previous reports on d(CGG) structure were mainly categorized into two forms, quadruplex and hairpin. Fry and Loeb (1994) reported CGG7 to form a bimolecular tetraplex from their DMS methylation protection experiment (Fry & Loeb 1994). On the other hand, Fojtík *et al.* (2004) considered CGG7 to form a bimolecular homoduplex and CGG16 a hairpin structure judged from CD spectra and their electrophoretic mobility on PAGE. The CD spectra reported by Fojtík *et al.* (2004) demonstrated a strong negative peak at 260 nm and a weak positive peak at 290 nm, being similar to ours and different from either a typical B structure or quadruplex. Interpretations that Fojtík *et al.* (2004) gave are as follows: CD spectra that they obtained represented a homoduplex and hairpin, and the difference from a typical B-structure could be derived from the winding of the DNA double helix because of high ionic strength. At present, we conclude the secondary structure of CGG16 is not a simple hairpin or quadruplex but some other non-B structure under physiologic-like conditions. However, it is reasonable to consider that the CD spectra we obtained in the present study for CGG16 indicate a formation of a hairpin having a non-B structured duplex.

Previously, CGG7 was reported to form a bimolecular quadruplex as described previously (Fry & Loeb 1994). However, it is demonstrated in the present study to form a non-B structure, being different from the quadruplex (Fig. 1B). $d(CGG)_8$ was also reported to form a bimolecular homoduplex (Fojtík *et al.* 2004). In any case, the d(CGG) repeat can form some bimolecular secondary structure when its repetitive number (n) is relatively small, being seven or eight. In contrast, the triplet repeat of CGG with 16 repetitive units, or even more, is able to form some unimolecular unusual higher structure, probably a hairpin having a stem deviating from a B-formed duplex. The formation of these peculiar DNA secondary structures could cause the arrest of DNA synthesis at the site leading to expansion of the repeat.

Some proteins of the RecQ helicase family, such as BLM helicase and WRN helicase, unwind quadruplex DNA (Sun *et al.* 1998, 1999; Fry & Loeb 1999; Mohaghegh *et al.* 2001). Especially, WRN helicase can unwind bimolecular quadruplexes of the d(CGG) repeat (Fry & Loeb 1999). In addition, several members of the hnRNP family were demonstrated to destabilize quadruplexes, and three of them, CBF-A, uqTBP25, and hnRNP A2, were reported to destabilize a bimolecular quadruplex of CGG7 (Weisman-Shomer *et al.* 2000; Khateb *et al.* 2004). We demonstrated previously that hnRNP A1/UP1 unfolds a unimolecular quadruplex of $d(TTAGGG)_4$ and $d(GGCAG)_5$. Similar results were also reported by Myers *et al.* (2003). In this study, we extended our research and revealed that UP1 unfolds the non-B structure of $d(CGG)_n$ and abrogates DNA synthesis arrests on $d(CGG)_n$ templates. UP1 was originally isolated from calf thymus as a single-stranded DNA-binding protein (Herrick & Alberts 1976), and later demonstrated to be a proteolytic product corresponding to the N-terminal 195 amino acids of 34 kDa hnRNP A1 containing the two RNA binding domains (Merrill *et al.* 1986). hnRNP A1 is a pre-mRNA binding protein and is suspected to be involved in pre-mRNA transport, protection, and splicing (Dreyfuss *et al.* 1993), as well as telomere maintenance (LaBranche *et al.* 1998). Although UP1 bound to single-stranded $d(TTAGGG)_n$ and $d(CAGGG)_n$ with a high affinity (Fukuda *et al.* 2002), only a small amount of stable complex between UP1 and the d(CGG) repeat could be detected by electrophoretic mobility shift assay (data not shown). In accordance with this observation, the real-time monitoring of interaction between UP1 and a $d(CGG)_{10}$ repeat by an SPR biosensor suggests that the association of UP1 to $d(CGG)_{10}$ is very quick and the dissociation of UP1 from the repeats is immediate after unfolding the unusual secondary structure of the repeat. The affinity of UP1 to $d(CGG)_{10}$ was on a similar level as that to pRandom40, a random 40-mer oligonucleotide (Table 1), while those to $d(TTAGGG)_8$ and $d(GGCAG)_8$ were higher (Fukuda *et al.* 2001, 2002; Table 1). In addition to our results, UP1 was previously reported to bind to single-stranded DNA with no significant base specificity (Nadler *et al.* 1991) and, on the other hand, to bind to single-stranded $d(TTAGGG)_n$ with a high affinity in other reports (LaBranche *et al.* 1998). Structural studies indicated that conserved RNP motifs of UP1 play a key role in specific interaction with AG dinucleotides of the d(TTAGGG) repeat (Ding *et al.* 1999; Myers *et al.* 2003). Taking these data together, it is plausible that UP1 binds to single-stranded DNA with two different binding modes, and UP1 interacts with d(CGG) repeats in a low sequence-specific mode, different from a high-affinity mode in the cases of d(TTAGGG) and d(GGCAG) repeats. In the case of *Escherichia coli* single-stranded DNA binding protein (SSB), detailed kinetic studies have been carried out

and have identified multiple DNA-binding modes and cooperation for the interaction of SSB with single-stranded (ss) DNA (Bujalowski & Lohman 1986; Kozlov & Lohman 2002; for review, see Lohman & Ferrari 1994). Although further detailed studies are necessary to clarify how UP1 recognizes d(CGG) and d(TTAGGG) repeats, it is possible that UP1 interacts with ssDNA in two different modes through different RNP motifs. As for the effect of UP1 on the non-B form of CGG16, UP1 does not have a prominent effect under a concentration of 150 mM KCl, but unfolds the secondary structure under a concentration of 0–15 mM KCl (Figs 2C and 4C). This data suggests that the non-B structure of the CGG16 under low concentrations of potassium ions may be unstable, and UP1 converts this unstable non-B structure into the B structure. Abrogation of the arrest of DNA synthesis on the $d(CGG)_n$ template by UP1 was also observed under a low concentration of KCl (15 mM), supporting the conversion of the non-B secondary structure of d(CGG) repeats into a single-stranded form by UP1. One of the possible explanations is that hnRNP A1/UP1 unfolds the secondary structure *in vivo* by cooperating with other proteins, such as WRN helicase. In fact, it was recently reported that hnRNP A1 has the domains of both positive and negative mediators for destabilization of a bimolecular quadruplex of $d(CGG)_n$, and a mutant hnRNP A1 deleted $RNP2_1$, the negative mediator domain, displays robust destabilization activity for a bimolecular quadruplex of CGG7 (Khateb *et al.* 2004). An intriguing scenario is that binding of some unknown proteins or smaller molecules to hnRNP A1/UP1 may thereby inhibit the function of negative mediators and enhance the destabilization activity of hnRNP A1/UP1 itself to unfold the secondary structure of $d(CGG)_n$, even in the presence of 150 mM KCl.

Our finding that UP1 has the activity to unfold the secondary structure of the d(CGG) repeat *in vitro* and to abrogate the pausings of DNA polymerase progression at the repeat suggests that UP1 may prevent the onset of Fragile X syndrome and other diseases implicated in the alteration of CGG or GCG repeats by inhibiting the expansion of this repeat *in vivo* through this activity. Further studies on mutation and expression of hnRNP A1/UP1 in Fragile X syndrome patients are indispensable to prove if this hypothesis is true.

Experimental procedures

Oligonucleotides

All synthetic oligonucleotides were purified by electrophoresis (Grainer Japan Co.). The names and nucleotide sequences of oligonucleotides are as follows: CGG7, $d(CGG)_7CGTGGACTC$; CGG16, $d(CGG)_{16}$; CGG16mut, $d(CGG)_5(AGG)(CGG)_4(AGG)(CGG)_5$. SubCGG16: dCGACTCTAGA$(CGG)_{16}$TGACTCTAGTACTGGCCGTCG TTTTACAACGTCG and its 3′-complementary 24 mer sequence pM13-20 were used for primer extension experiments.

Expression and purification of recombinant UP1

UP1 was expressed in *E. coli* XL1-Blue as a GST-fusion protein and purified as previously described (Fukuda *et al.* 2002). All purification steps were monitored by electrophoretic mobility-shift assay and SDS-polyacrylamide gel electrophoresis.

CD analysis

For CD measurement, lyophilized DNA, CGG7, and CGG16, were dissolved in 20 mM sodium phosphate buffer (pH 7.0) containing 150 mM KCl. The strand concentration was 10 μM. Each sample was heated at 90 °C for 5 min, followed by gradual cooling to room temperature, and stored at 4 °C until use. Either GST-UP1 or GST, dissolved in 20 mM sodium phosphate buffer (pH 7.0) containing 1 mM EDTA, 1 mM DTT, 1 mM PMSF, 1 mM benzamidine, and 0.2% acetone, was added step by step to each DNA sample with DNA to protein ratios of 1 : 0.5, 1 : 1, and 1 : 2. CD spectra of the DNA and DNA-protein complexes were recorded with a Jasco J-720 spectropolarimeter and a 1 mm cell. CD spectra of GST-UP1 and GST were also recorded. From the CD spectrum obtained for the DNA-protein complex, the spectrum for the corresponding protein was subtracted.

Protein-DNA interaction analysis by SPR-based biosensor

Binding experiments were performed by monitoring the association and dissociation reactions in real time using an SPR biosensor, BIACORE3000 system. GST-UP1 was diluted to various concentrations with HBS-EP buffer [10 mM HEPES (pH 7.4), 150 mM NaCl, 3 mM EDTA, 0.005% Tween 20 (pH 7.4)] or the HBS-EP buffer containing 15 mM NaCl, and injected in the oligonucleotide-immobilized sensor chip at a constant flow rate of 20 μL/min. The kinetic parameters of the interactions were calculated by non-linear curve fitting analysis of the association and dissociation curves using BIA evaluation version 3.0 software (Biacore).

In vitro DNA synthesis assay

A primer extension reaction was performed as previously described (Fukuda *et al.* 2002) with some modifications. A mixture of the pSubCGG16 and the pM13-20 primer, which was labeled with ^{32}P at the 5′ end (final 100 nM each), in TE buffer containing 150 mM KCl was heated at 95 °C for 5 min and then at 72 °C for 5 min, followed by gradual cooling, and incubated at 37 °C for 3 h. An aliquot of 0.75 μL of this primer-annealed template was mixed with 0.75 μL of 10× *Bca*BEST buffer [200 mM

Tris-HCl (pH 8.5), 100 mM $MgCl_2$] and 0.5 μL of dNTPs mixture (50 μM each). After adding 1 μL of the GST-UP1 suspended in buffer P [20 mM sodium phosphate (pH 7.0), 0.5 mM DTT], the mixture was incubated at 37 °C for 5 min, and then the primer extension reaction was carried out at 37 °C for 8 min in the presence of *Bca*BEST DNA polymerase (final 66 U/mL, Takara Biomedicals). The concentrations of *Bca*BEST DNA polymerase, the primer-annealed template, and dNTPs were 18 U/mL, 10 nM, and 1.7 μM, respectively. The reaction was terminated by adding 1.5 μL of stop solution (160 mM EDTA, 0.7% SDS, 6 mg/mL proteinase K), and then the samples were incubated at 37 °C for 30 min. A primer extension reaction using DNA polymerase α was performed as described previously with some modifications. Human DNA polymerase α (Chimerx) 0.2 units were used per reaction. The reaction solution was as follows; 50 mM Tris-HCl (pH 7.5), 5 mM $MgCl_2$, 2 mM DTT, 250 μg/mL BSA, dNTPs mixture (10 μM each). The reaction time for primer extension was 20 min.

Acknowledgements

This work was supported by a Grant-in-Aid for Cancer Research from the Ministry of Health, Labor and Welfare of Japan, and Grants-in-Aid for Scientific Research (Nos.15030214 and 16048209 for M.K., No.15570131 for H.F.) and the Protein 3000 Project (for M.K.) from the Ministry of Education, Culture, Sports, Science, and Technology of Japan. H.F. was supported by a Research Grant of the Princess Takamatsu Cancer Research Fund, and the Senri Life Science Foundation. We thank Professor S. Uesugi (Yokohama Natl. University) and Dr T. Sugimura (National Cancer Center Research Institute) for helpful discussions.

References

Bujalowski, W. & Lohman, T.M. (1986) *Escherichia coli* single-strand binding protein forms multiple, distinct complexes with single-stranded DNA. *Biochemistry* **25**, 7799–7802.

Chen, X., Mariappan, S.V., Catasti, P., *et al.* (1995) Hairpins are formed by the single DNA strands of the fragile X triplet repeats: structure and biological implications. *Proc. Natl. Acad. Sci. USA* **92**, 5199–5203.

Crawford, D.C., Acuna, J.M. & Sherman, S.L. (2001) FMR1 and the fragile X syndrome: human genome epidemiology review. *Genet. Med.* **3**, 359–371.

Dapic, V., Abdomerovic, V., Marrington, R., *et al.* (2003) Biophysical and biological properties of quadruplex oligodeoxyribonucleotides. *Nucleic Acids Res.* **31**, 2097–2107.

Ding, J., Hayashi, M.K., Zhang, Y., *et al.* (1999) Crystal structure of the two-RRM domain of hnRNP A1 (UP1) complexed with single-stranded telomeric DNA. *Genes Dev.* **13**, 1102–1115.

Dreyfuss, G., Matunis, M.J., Pionl-Roma, S. & Burd, C.G. (1993) hnRNP proteins and the biogenesis of mRNA. *Annu. Rev. Biochem.* **269**, 289–321.

Fojtík, P., Kejnovská, I. & Vorlíčková, M. (2004) The guanine-rich fragile X chromosome repeats are reluctant to form tetraplexes. *Nucleic Acids Res.* **32**, 298–306.

Fry, M. & Loeb, L.A. (1994) The fragile X syndrome $d(CGG)_n$ nucleotide repeats form a stable tetrahelical structure. *Proc. Natl. Acad. Sci. USA* **91**, 4950–4954.

Fry, M. & Loeb, L.A. (1999) Human Werner syndrome DNA helicase unwinds tetrahelical structures of the fragile X syndrome repeat sequence $d(CGG)_n$. *J. Biol. Chem.* **274**, 12797–12802.

Fukuda, H., Sugimura, T., Nagao, M. & Nakagama, H. (2001) Detection and isolation of minisatellite Pc-1 binding proteins. *Biochim. Biophys. Acta* **1528**, 152–158.

Fukuda, H., Katahira, M., Tsuchiya, N., *et al.* (2002) Unfolding of quadruplex structure in the G-rich strand of the minisatellite repeat by the binding protein UP1. *Proc. Natl. Acad. Sci. USA* **99**, 12685–12690.

Gacy, A.M., Goellner, G., Juranic, N., *et al.* (1995) Trinucleotide repeats that expand in human disease form hairpin structures *in vitro*. *Cell* **81**, 533–540.

Herrick, G. & Alberts, B. (1976) Purification and physical characterization of nucleic acid helix-unwinding proteins from calf thymus. *J. Biol. Chem.* **251**, 2124–2132.

Kamath-Loeb, A.S., Loeb, L.A., Johansson, E., *et al.* (2001) Interactions between the Werner syndrome helicase and DNA polymerase delta specifically facilitate copying of tetraplex and hairpin structures of the $d(CGG)_n$ trinucleotide repeat sequence. *J. Biol. Chem.* **276**, 16439–16446.

Kang, S., Ohshima, K., Shimizu, M., *et al.* (1995) Pausing of DNA synthesis *in vitro* at specific loci in CTG and CGG triplet repeats from human hereditary disease genes. *J. Biol. Chem.* **270**, 27014–27021.

Kettani, A., Kumar, R.A. & Patel, D.J. (1995) Solution structure of a DNA quadruplex containing the fragile X syndrome triplet repeat. *J. Mol. Biol.* **254**, 638–656.

Khateb, S., Weisman-Shomer, P., Hershco, I., *et al.* (2004) Destabilization of tetraplex structures of the fragile X repeat sequence $(CGG)_n$ is mediated by homolog-conserved domains in three members of the hnRNP family. *Nucleic Acids Res.* **32**, 4145–4154.

Kozlov, A.G. & Lohman, T.M. (2002) Kinetic mechanism of direct transfer *Escherichia coli* SSB tetramer between single-stranded DNA molecules. *Biochemistry* **41**, 11611–11627.

LaBranche, H., Dupuis, S., Ben-David, Y., *et al.* (1998) Telomere elongation by hnRNP A1 and a derivative that interacts with telomeric repeats and telomerase. *Nature Genet.* **19**, 199–202.

Lohman, T.M. & Ferrari, M.E. (1994) *Escherichia coli* single-stranded DNA-binding protein: multiple DNA-binding modes and cooperativities. *Annu. Rev. Biochem.* **63**, 527–570.

Mandel, J.L. (1993) Questions of expansion. *Nature Genet.* **4**, 8–9.

Merrill, B.M., LoPresti, M.B., Stone, K.L. & Williams, K.R. (1986) High pressure liquid chromatography purification of UP1 and UP2, two related single-stranded nucleic acid-binding protein from calf thymus. *J. Biol. Chem.* **261**, 878–883.

Mohaghegh, P., Karow, J.K., Brosh Jr., R.M., *et al.* (2001) The Bloom's and Werner's syndrome proteins are DNA structure-specific helicases. *Nucleic Acids Res.* **29**, 2843–2849.

Myers, J.C., Moore, S.A. & Shamoo, Y. (2003) Structure-based incorporation of 6-methyl-8-(2-deoxy-β-ribofuranosyl) isoxanthopteridine into the human telomeric repeat DNA as a

probe for UP1 binding and destabilization of G-tetrad structures. *J. Biol. Chem.* **278**, 42300–42306.

Nadel, Y., Weisman-Shomer, P. & Fry, M. (1995) The fragile X syndrome single strand d(CGG)n nucleotide repeats readily fold back to form unimolecular hairpin structures. *J. Biol. Chem.* **270**, 28970–28977.

Nadler, S.G., Merrill, B.M., Roberts, W.J., *et al.* (1991) Interactions of the A1 heterogeneous nuclear ribonucleoprotein and its proteolytic derivative, UP1, with RNA and DNA: evidence for multiple RNA binding domains and salt-dependent binding mode transitions. *Biochemistry* **30**, 2968–2976.

Rousseau, F., Heitz, D. & Mandel, J.L. (1992) The unstable and methylatable mutations causing the fragile X syndrome. *Hum. Mutat.* **1**, 91–96.

Samadashwily, G.M., Raca, G. & Mirkin, S.M. (1997) Trinucleotide repeats affect DNA replication *in vivo*. *Nature Genet.* **17**, 298–304.

Sun, H., Karow, J.K., Hickson, I.D. & Maizels, N. (1998) The Bloom's syndrome helicase unwinds G4 DNA. *J. Biol. Chem.* **273**, 27587–27592.

Sun, H., Bennett, R.J. & Maizels, N. (1999) The *Saccharomyces cerevisiae* Sgs1 helicase efficiently unwinds G-G paired DNAs. *Nucleic Acids Res.* **27**, 1978–1984.

Usdin, K. & Woodford, K.J. (1995) CGG repeats associated with DNA instability and chromosome fragility form structures that block DNA synthesis *in vitro*. *Nucleic Acids Res.* **23**, 4202–4209.

Weisman-Shomer, P., Naot, Y. & Fry, M. (2000) Tetrahelical forms of the fragile X syndrome expanded sequence d(CGG)(n) are destabilized by two heterogeneous nuclear ribonucleoprotein-related telomeric DNA-binding proteins. *J. Biol. Chem.* **275**, 2231–2238.

Received: 21 April 2005
Accepted: 10 July 2005

Carcinogenesis vol.27 no.1 pp.162–169, 2006
doi:10.1093/carcin/bgi205
Advance Access publication August 4, 2005

Strain differences in the susceptibility to azoxymethane and dextran sodium sulfate-induced colon carcinogenesis in mice

Rikako Suzuki*, Hiroyuki Kohno, Shigeyuki Sugie, Hitoshi Nakagama[1] and Takuji Tanaka

Department of Oncologic Pathology, Kanazawa Medical University, 1-1 Daigaku, Uchinada, Ishikawa 920-0293, Japan and [1]Biochemistry Division, National Cancer Center Research Institute, 5-1-1 Tsukiji Chuo-ku, Tokyo 104-0045, Japan

*To whom correspondence should be addressed. Tel: +81 76 286 2211; Fax: +81 76 286 6926; E-mail: rikako@kanazawa-med.ac.jp

We have recently developed a mouse model for colitis-related colon carcinogenesis by a combined treatment with azoxymethane (AOM) and dextran sodium sulfate (DSS) in male ICR mice. However, strain differences in the sensitivity to AOM/DSS-induced colon carcinogenesis in mice have yet to be elucidated. The aim of this study was to determine the presence of any genetically determined differences in sensitivity to our model of colon carcinogenesis in four inbred strains of mice. Male Balb/c, C3H/HeN, C57BL/6N and DBA/2N mice were given a single intraperitoneal injection of AOM (10 mg/kg body wt), followed by 1% DSS (w/v) in drinking water for 4 days, and thereafter they received no further treatment for up to 16 weeks. At the end of the study (Week 18), all mice were killed and a histopathological analysis of their colon was performed. The incidence of colonic adenocarcinoma was 100% with a multiplicity (no. of tumors/mouse) of 7.7 ± 4.3 in the Balb/c mice and 50% with a multiplicity of 1.0 ± 1.2 in the C57BL/6N mice. On the other hand, only a few colonic adenomas, but no adenocarcinomas, developed in the C3H/HeN mice (29% incidence with a multiplicity of 0.7 ± 1.5) and the DBA/2N mice (20% incidence with a multiplicity of 0.2 ± 0.4). The inflammation and immunohistochemical nitrotyrosine-positivity scores of the mice treated with AOM and DSS in the decreasing order were as follows: C3H/HeN > Balb/c > DBA/2N > C57BL/6N and Balb/c > C57BL/6N > C3H/HeN > DBA/2N, respectively. Our results thus indicated the presence of strain differences in the susceptibility to AOM/DSS-induced colonic tumorigenesis. These differences may have been directly influenced by the response to nitrosation stress due to the inflammation caused by DSS.

Introduction

Colorectal cancer (CRC) is one of the most common malignant neoplasms in both sexes (1). In Western countries, this malignancy is one of the most leading causes of cancer deaths (1). In patients with inflammatory bowel disease (IBD), including ulcerative colitis (UC) and Crohn's disease, the risk of CRC development is higher than in the general population (2–5). In sporadic and IBD-related CRC, the expression of inducible nitric oxide synthase and cyclooxygenase-2, both of which are associated with inflammation, has been reported to be elevated (6,7). As a result, inflammation is suggested to play an important role in IBD-related CRC (2).

In our recent series of studies on inflammation-related colon carcinogenesis, we developed a novel model of colitis-related colon carcinogenesis using ICR mice. In this animal model, ICR mice received a single dose of a different colonic carcinogen, consisting of either azoxymethane (AOM) (8), 2-amino-1-methyl-6-phenylimidazo[4,5-*b*]pyridine (9) or 1, 2-dimethylhydrazine (10), followed by a 1-week exposure to 2% dextran sodium sulfate (DSS) in their drinking water, which thus resulted in a high incidence of colonic epithelial malignancy within 20 weeks (8–10). We have previously proposed that the colonic inflammation and nitrosative stress caused by DSS exposure contributes to the development of cryptal dysplasia and neoplasms in the colon (8–10).

AOM is a colonic genotoxic carcinogen that is extensively used for the investigation of large bowel carcinogenesis in rodents (11–13). A synthetic sulfate polysaccharide, DSS, is a non-genotoxic colonic carcinogen that is widely used to produce colitis in rodents, which shares most features with human UC (14–18). It is well known that different strains of mice have different sensitivities to xenobiotic including AOM and DSS (19–28). For example, the Balb/CJ strain is known to be susceptible to AOM (26), whereas, the C3H (29), C57BL/6J (26) and DBA/2 (25) strains are less sensitive to AOM. Regarding the sensitivity to DSS in several mouse strains, Balb/c, C3H/HeJ, and C57BL/6J mice are relatively susceptible to DSS, while DBA/2J mice have been reported to be virtually resistant (27,28). It may therefore be possible that the differences in the genetic background of the mice differently affect the colon carcinogenesis induced by AOM and DSS.

The current study was conducted to determine the different sensitivities to AOM/DSS-induced colon carcinogenesis in four different inbred mouse strains, namely Balb/c, C3H/HeN, C57BL/6N and DBA/2N, by evaluating the incidence and multiplicity of colonic tumors. In addition, an immunohistochemical analysis of nitrotyrosine, a marker of both formation of peroxynitrite (30) and perhaps the inflammation-associated carcinogenesis (31), was done to evaluate whether nitrosative stress is involved in the strain difference sensitivity to AOM/DSS-induced colon tumorigenesis.

Materials and methods

Animals, chemicals and diets

For the study 5-week-old male mice of Balb/c, C3H/HeN, C57BL/6N and DBA/2N strains were obtained from Charles River Japan, (Tokyo, Japan). AOM was purchased from the Sigma-Aldrich (St Louis, MO). DSS with a molecular weight of 36 000–50 000 was purchased from ICN Biochemicals,

Abbreviations: AOM, azoxymethane; CRC, colorectal cancer; CYP, Cytochrome P450; DSS, dextran sodium sulfate; IBD, inflammatory bowel disease; IKK, IκB kinase; LPS, lipopolysaccharide; UC, ulcerative colitis.

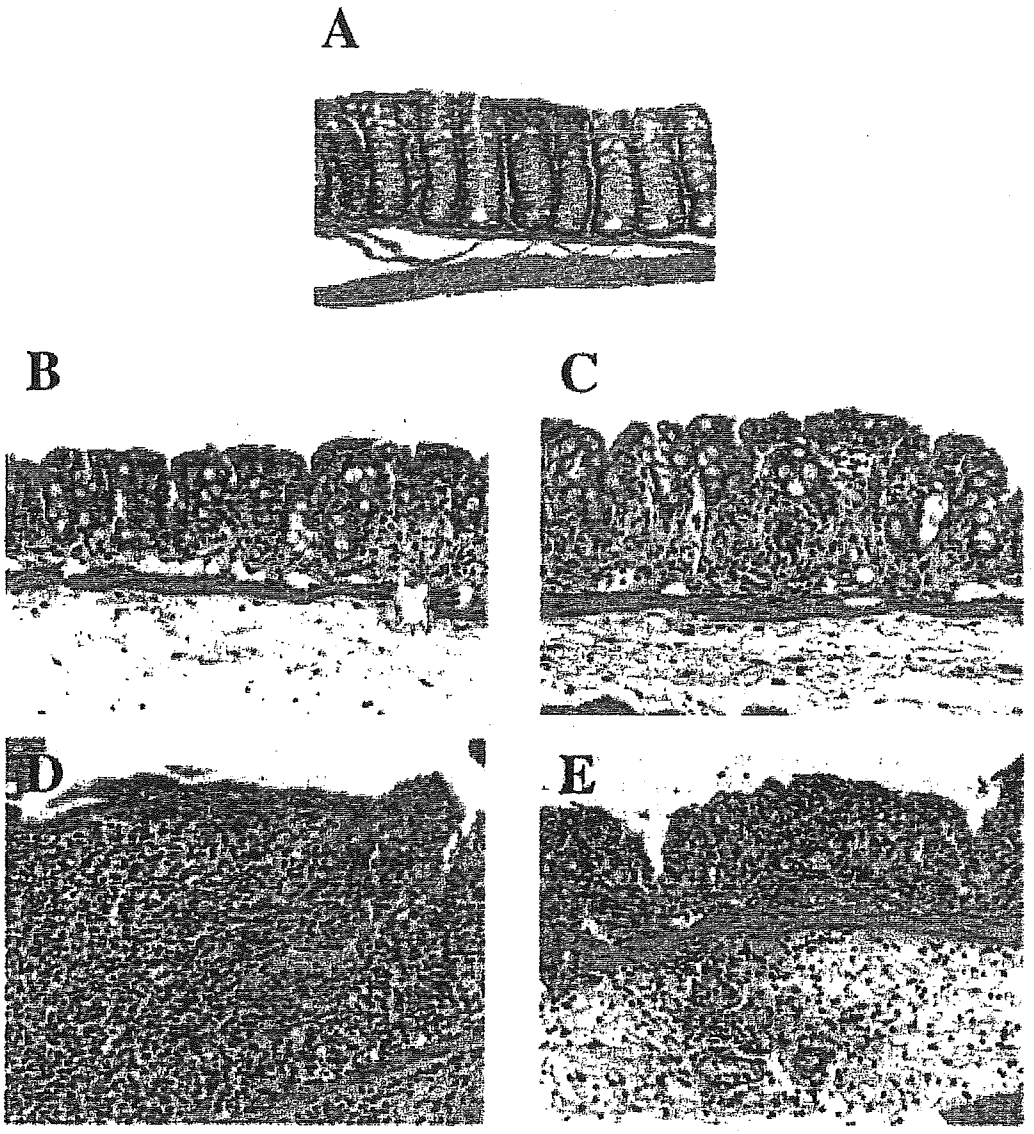

Fig. 1. Various grades of colitis. (**A**) Normal colon mucosa (Grade 0); (**B**) shortening the basal one-third of the crypts with slight inflammation and edema in the lamina propria (Grade 1); (**C**) loss of the basal two-thirds of the crypts with moderate inflammation in the lamina propria (Grade 2); (**D**) loss of all the crypts with severe inflammation in the lamina propria, but with the surface epithelium still remaining (Grade 3); and (**E**) a loss of all the crypts and surface epithelium with severe inflammation in the mucosa, muscularis propria and submucosa. An exudate containing cell debris, inflammatory cells, fibrin and mucus covers the damaged mucosa (Grade 4). Hematoxylin and eosin stain. Original magnification, (A–E), 20×.

(Cat. No. 160110, Aurora, OH). CRF-1 (Oriental Yeast, Tokyo, Japan) was used as the basal diet throughout the study.

Experimental procedure

After they were brought, the mice were acclimated for 1 week with tap water and a pelleted basal diet, CRF-1, *ad libitum*. The experimental groups in each strain of mice included the AOM and DSS group, the AOM alone group, the DSS alone group and the untreated control group. The experimental protocol in the current study was slightly modified from our original protocol (8). We chose 1% as the dose level of DSS since this dose has been shown to exert sufficient tumor-promoting effects (32). In addition, the duration (4 days) of DSS exposure in drinking water was shortened based on our preliminary investigation, in which 4 days of exposure to DSS was found to enhance AOM-initiated colon carcinogenesis in ICR mice of either sex. All mice were maintained at the Kanazawa Medical University Animal Facility according to the Institutional Animal Care Guidelines, and were maintained under controlled conditions of humidity (50 ± 10%), light (12/12 h light/dark cycle) and temperature (23 ± 2°C).

Histopathological analysis

At the end of the experiment (Week 18), all the mice were killed by an ether overdose. At autopsy, their large bowel was flushed with saline and excised. After measuring the length of the large bowel (from the ileocecal junction to the anal verge), it was cut open longitudinally along the main axis and washed with saline. The large bowel was then carefully inspected for the presence of pathological lesions and fixed in 10% buffered formalin for at least 24 h. Paraffin-embedded sections of the large bowel were then made by routine procedures. Any histopathological alterations in the colon were examined on hematoxylin and eosin-stained sections. Colitis was recorded and scored according to the following morphological criteria described by Cooper *et al.* (33): Grade 0 (Figure 1A), normal colonic mucosa; Grade 1 (Figure 1B), shortening and loss of the basal one-third of the actual crypts with mild inflammation and edema in the mucosa: Grade 2 (Figure 1C), loss of the basal two-thirds of the crypts with moderate inflammation in the mucosa; Grade 3 (Figure 1D), loss of all crypts with severe inflammation in the mucosa, but with the surface epithelium still remaining; and Grade 4 (Figure 1E), loss

of all crypts and the surface epithelium with severe inflammation in the mucosa, muscularis propria and submucosa. Intestinal neoplasms were diagnosed according to the criteria described by Pozharisski (34).

Immunohistochemistry

Nitrotyrosine immunohistochemistry was carried out on 4-μm-thick paraffin-embedded sections from the colons in all four strains of mice administered 1% DSS alone as previously described (8,35). The deparaffinized sections were incubated overnight with a primary rabbit polyclonal anti-nitrotyrosine (diluted 1:1500, CHEMICON International, CA) or with a control solution. Control sections included buffer alone or non-specific purified rabbit secondary antibody and avidin–biotin-peroxidase complex (Vectastain Elite ABC kit, Vector Laboratories, Burlingame, CA). The color was developed using 3,3′-diaminobenzidine-4HCl as the chromogen. The stained sections were examined for the localization and intensity of immunoreactivity by microscopy (Olympus AX70, Olympus Optical, Tokyo, Japan). To the degree of nitrotyrosine stainability, the following grading system (Grade 0–4) was applied: Grade 0, no immunoreactivity and no positive cells; Grade 1, weak immunoreactivity and <10% positive cells; Grade 2, mild immunoreactivity and 10–30% positive cells; Grade 3, moderate immunoreactivity and 31–60% positive cells; and Grade 4, strong immunoreactivity and 61–100% positive cells with extensive immunoreactivity (36).

Statistical analysis

Where applicable, the data were analyzed using one-way ANOVA with either Bonferroni correction or Fisher's exact probability test (GraphPad Instat version 3.05, GraphPad Software, San Diego, CA), with $P < 0.05$ as the criterion of significance.

Results

General observation

The intake of DSS-containing tap water did not significantly differ among the four strains of mice (data not shown). Mice that received AOM and 1% DSS or 1% DSS alone demonstrated bloody stools either during DSS administration or soon after the cessation of DSS exposure. The degree of this symptom varied among the strains: Balb/c and C3H/HeN mice showed severe symptoms while C57BL/6N and DBA/2N mice showed mild symptoms. The mean body weight and colon length of the mice are summarized in Table I. The mean body weight of the Balb/c mice, which received AOM/DSS, was significantly lower than that of the C3H/HeN mice ($P < 0.01$) and C57BL/6N mice ($P < 0.01$), which were given AOM and DSS. A significant difference on the mean body weight was found between the AOM/DSS group and the untreated group ($P < 0.001$) in Balb/c mice. As listed in Table I, the mean lengths of the colon in the Balb/c mice ($P < 0.001$) and C3H/HeN mice ($P < 0.001$) that were treated with AOM/DSS were statistically longer than in the C57BL/6N mice. A significant difference ($P < 0.001$) was also observed between the C57BL/6N and DBA/2N mice that were exposed to AOM/DSS. The C57BL/6N mice given AOM alone has a significantly shorter colon than the Balb/c ($P < 0.01$) and DBA/2N mice ($P < 0.01$) treated with AOM alone. As for the untreated group, the colon length of the C57BL/6N mice was significantly shorter than that of the Balb/c ($P < 0.01$) and DBA/2N mice ($P < 0.01$).

Incidence and multiplicity of large bowel neoplasms

Macroscopically, colonic neoplasms developed with a different incidence and multiplicity for each strain of mice that received AOM and 1% DSS. Flat, nodular, polypoid or caterpillar-like tumors were mainly located in the middle and/or distal colon if any tumors existed (Figure 2). Histopathologically, they were tubular adenoma (Figure 3A) or adenocarcinoma (Figure 3B). Dysplastic lesions were also observed in the colonic mucosa surrounding the tumors. None of the strains of mice given AOM alone, 1% DSS alone or tap water had any colonic tumors.

Table I. Body and relative liver weights and lengths of colon in each strain of mice

Strain	Treatment (no. of mice examined)	Body weight (g)	Length of colon (cm)
Balb/c	AOM→1% DSS (10)	25.1 ± 3.8[a,b,c,d]	12.7 ± 1.0[e]
	AOM (4)	30.9 ± 0.8	14.0 ± 1.0[f]
	1% DSS (5)	34.1 ± 2.0	13.0 ± 0.6
	None (5)	32.4 ± 1.1	13.7 ± 0.5[g]
C3H/HeN	AOM→1% DSS (7)	30.2 ± 0.6	12.7 ± 1.3[e]
	AOM (5)	32.6 ± 2.2	12.5 ± 0.6
	1% DSS (5)	32.2 ± 1.2	13.1 ± 1.1
	None (3)	31.8 ± 1.1	11.9 ± 0.6
C57BL/6N	AOM→1% DSS (10)	29.3 ± 1.9	11.1 ± 0.6[h]
	AOM (5)	31.3 ± 2.0	11.7 ± 0.5[i]
	1% DSS (5)	32.0 ± 1.7	12.8 ± 0.9
	None (5)	33.0 ± 4.7	11.6 ± 1.0[j]
DBA/2N	AOM→1% DSS (10)	28.3 ± 2.3	13.2 ± 1.0
	AOM (5)	28.9 ± 1.3	14.1 ± 0.9
	1% DSS (5)	30.5 ± 0.6	14.0 ± 0.8
	None (5)	30.7 ± 1.4	13.6 ± 1.7

[a]Mean ± SD.
[b]Significantly different from untreated Balb/c mice ($P < 0.001$).
[c]Significantly different from C3H/HeN mice which received AOM/DSS ($P < 0.01$).
[d]Significantly different from C57BL/6N mice which received AOM/DSS ($P < 0.01$).
[e]Significantly different from C57BL/6N mice which received AOM/DSS ($P < 0.001$).
[f]Significantly different from C57BL/6N mice which received AOM alone ($P < 0.01$).
[g]Significantly different from untreated C57BL/6N mice ($P < 0.01$).
[h]Significantly different from DBA/2N mice which received AOM/DSS ($P < 0.001$).
[i]Significantly different from DBA/2N mice which received AOM alone ($P < 0.01$).
[j]Significantly different from untreated DBA/2N mice ($P < 0.01$).

The incidence (percent of mice with tumors) of colonic neoplasms is summarized in Figure 4A. The incidence of colonic neoplasms in the Balb/c mice (100%) was significantly higher than in the C3H/HeN mice (29%, $P = 0.0034$) and the DBA/2N mice (20%, $P = 0.0004$). A statistically significant difference ($P = 0.0115$) was also noted between the C57BL/6N (80%) and the DBA/2N mice. The order of the incidence of colonic adenoma was Balb/c mice (90%) > C57BL/6N mice (70%) > C3H/HeN mice (29%) > DBA/2N mice (20%). The incidence of adenoma in Balb/c mice was statistically greater than in C3H/HeN mice ($P = 0.0175$) and DBA/2N mice ($P = 0.0027$), and the difference between C57BL/6N mice and DBA/2N mice was statistically significant ($P = 0.0349$). The incidence of colonic adenocarcinoma was 100% in the Balb/c mice and 50% in the C57BL/6N mice and a statistically significant difference ($P = 0.0163$) was found between these two strains of mice. However, this malignancy was not found in the C3H/HeN and DBA/2N mice. As shown in Figure 4B, the multiplicity of colonic neoplasms (/mouse) was 11.4 ± 5.9 in Balb/c mice, 0.7 ± 1.5 in C3H/HeN mice, 2.5 ± 2.1 in C57BL/6N mice and 0.2 ± 0.4 in DBA/2N mice. The value for the Balb/c mice was significantly higher ($P < 0.001$) than that of other strains of mice. The order of the multiplicity of adenoma was Balb/c mice (3.7 ± 3.3) > C57BL/6N mice (1.5 ± 1.3) > C3H/HeN mice (0.7 ± 1.5) > DBA/2N mice (0.2 ± 0.4). The value for multiplicity of adenoma in the Balb/c mice was statistically greater than in the C3H/HeN

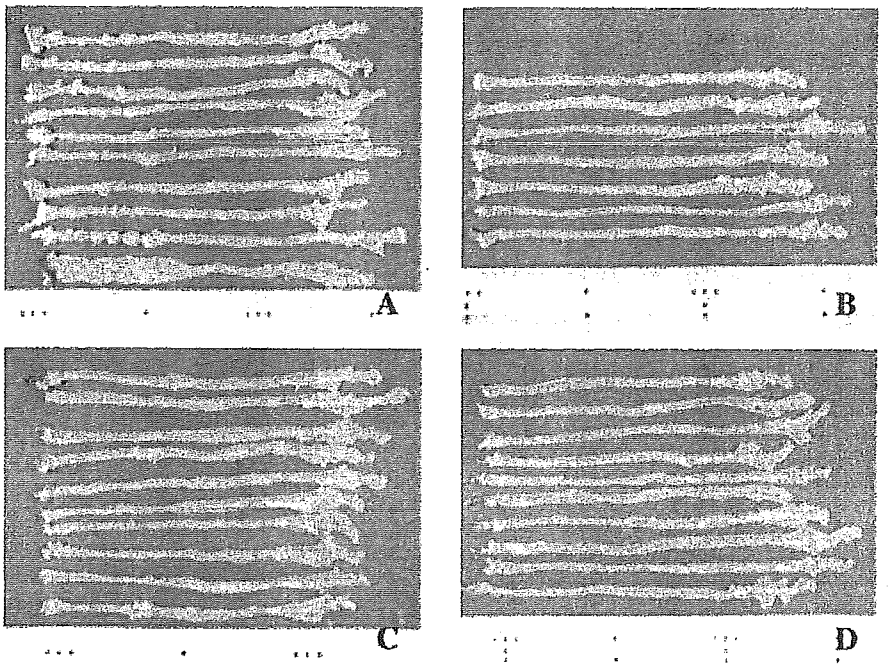

Fig. 2. Macroscopic view of the large bowel treated with AOM and 1% DSS. (**A**) Numerous colon tumors (2–21 tumors per mouse) develop in all Balb/c mice. (**B**) One or four colonic tumors are seen in two out of seven C3H/HeN mice. (**C**) One to five colonic tumors are found in 8 out of 10 C57BL/6N mice. (**D**) One colonic tumor is present in 2 out of 10 DBA/2N mice.

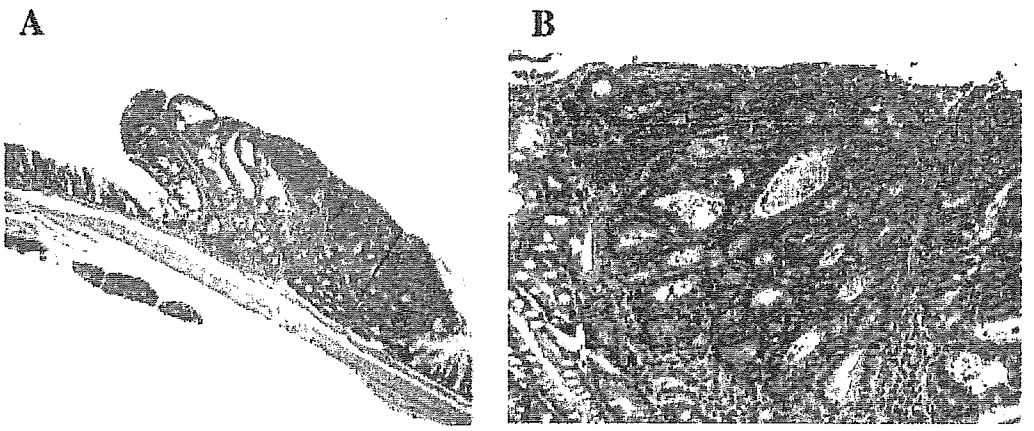

Fig. 3. Histopathology of colonic neoplasms in male Balb/c mice treated with AOM and 1% DSS. (**A**) Tubular adenoma and (**B**) moderately-differentiated adenocarcinoma. Hematoxylin and eosin stain. Original magnification, A, 2× and B, 20×.

mice ($P < 0.05$) and DBA/2N mice ($P < 0.01$). The multiplicity of adenocarcinoma in the Balb/c mice (7.7 ± 4.3) was the greatest among the four strains and it was significantly larger than that in the C3H/HeN mice (1.0 ± 1.2, $P < 0.001$).

The scores of inflammation and nitrotyrosine

As shown in Figure 5, the inflammation scores of each strain of mice initiated with AOM and followed by DSS exposure were 1.2 ± 1.1 in Balb/c, 2.3 ± 1.3 in C3H/HeN, 0.4 ± 0.7 in C57BL/6N and 0.6 ± 0.7 in DBA/2N, respectively. The score of C3H/HeN was significantly greater than that for C57BL/6N ($P<0.01$) and DBA/2N ($P<0.01$). As for the mice that received 1% DSS alone, the inflammation score of the C3H/HeN mice (1.4 ± 0.5) was the highest among the strains (1.0 ± 1.2 in Balb/c mice and 0.2 ± 0.4 in DBA/2N mice). C57BL/6N mice given 1% DSS alone had quite a low score of inflammation. The mice treated with AOM alone and the untreated mice demonstrated extremely weak inflammation in the colon.

Nitrotyrosine immunoreactivity was mainly observed in the neoplastic cells, cryptal cells, blood endothelial cells and mononuclear cells, which infiltrated the colonic mucosa (Figure 6). The stainability was relatively weak for infiltrative mononuclear cells in comparison with the cryptal cells and endothelial cells (Figure 6). As shown in Figure 7, the nitrotyrosine immunohistochemistry findings for the Balb/c mice (3.6 ± 0.5) treated with AOM and DSS were significantly higher than those for C3H/HeN (1.7 ± 0.8, $P<0.001$) and DBA/2N mice (1.6 ± 0.5, $P<0.001$). The score of nitrotyrosine-positivity in C57BL/6N mice (3.4 ± 0.5) was

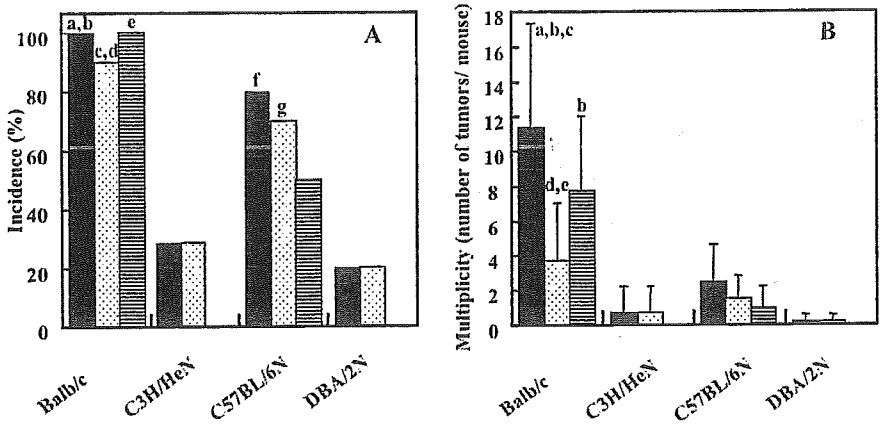

Fig. 4. Incidence and multiplicity of colonic tumors. (A) Incidence of colonic tumors. Black columns represent total; white column filled with dots represent adenoma and striped columns represent adenocarcinoma. a, Significantly different from C3H/HeN (P=0.0034); b, significantly different from DBA/2N (P = 0.0004); c, significantly different from C57BL/6N (P=0.0175); d, significantly different from DBA/2N (P=0.0027); e, significantly different from C57BL/6N (P=0.0163); f, significantly different from DBA/2N (P=0.0115); and g, significantly different from DBA/2N (P=0.0349). (B) Multiplicity of colonic tumors. Values are the mean ± SD. Black columns represent total; white column filled with dots represent adenoma and striped columns represent adenocarcinoma. a, Significantly different from C3H/HeN ($P<0.001$); b, significantly different from C57BL/6N ($P<0.001$); c, significantly different from DBA/2N ($P<0.001$); d, significantly different from C3H/HeN ($P<0.05$); and e, significantly different from DBA/2N ($P<0.01$).

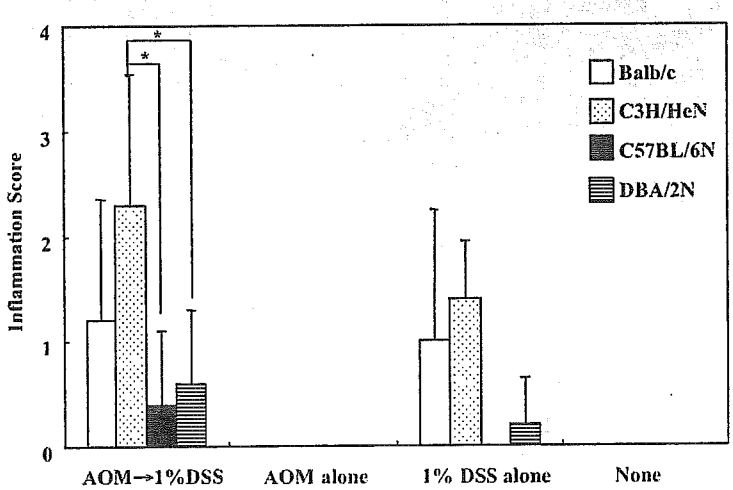

Fig. 5. Inflammation score in the colon for four strains of mice. Values are the mean ± SD. white column, Balb/c; white column with dots, C3H/HeN; black columns, C57BL/6N; striped columns, DBA/2N. *$P<0.01$.

statistically higher than those in C3H/HeN ($P < 0.001$) and DBA/2N ($P<0.001$) mice. In mice that received 1% DSS alone, the scores in Balb/c (2.8 ± 0.8) and C57BL/6N (2.4 ± 1.1) mice were higher than those in C3H/HeN (1.6 ± 0.5) and DBA/2N mice (1.4 ± 0.5); however, no significant differences were observed among the strains. As for the mice given AOM alone, the scores of nitrotyrosine in the Balb/c mice and C57BL/6N mice were 0.5 ± 0.6 and 0.2 ± 0.4, respectively. C3H/HeN mice and DBA/2N mice treated with AOM alone showed either no or faint stainability of nitrotyrosine. The degree of nitrotyrosine stainability in untreated mice was almost null.

Discussion

The present investigation demonstrated the different susceptibilities of the four strains (Balb/c, C3H/HeN, C57BL/6N and DBA/2N) of mice to colon tumorigenesis induced by the combination treatments with AOM and DSS. Apparently, Balb/c mice were extremely sensitive to AOM/DSS-induced colon carcinogenesis in the present experimental condition. The sensitivity of Balb/c mice observed in the present study was almost similar to those found in ICR mice (8,32,35). Colonic adenocarcinoma also developed in C57BL/6N, but the incidence was lower than in Balb/c. In contrast, the susceptibility of C3H/HeN and DBA/2N to the administration of AOM and DSS was quite low and only a few colonic adenomas developed in both the strains of mice.

Regarding the sensitivity of the mice to AOM initiation, the Balb/CJ mice were reported to have a remarkable susceptibility to the formation of distal colon tumors after treatment with AOM (26), whereas C3H, C57BL/6J, and DBA/2 mice were found to have a low incidence of colonic tumors by AOM initiation (25,26,29). Strain differences in the susceptibility to DSS have also been demonstrated: Balb/c, C3H/HeJ and C57BL/6J are relatively susceptible to DSS, whereas DBA/2J mice are virtually resistant based on the frequency of ulceration or the histological score of inflammation in the colon

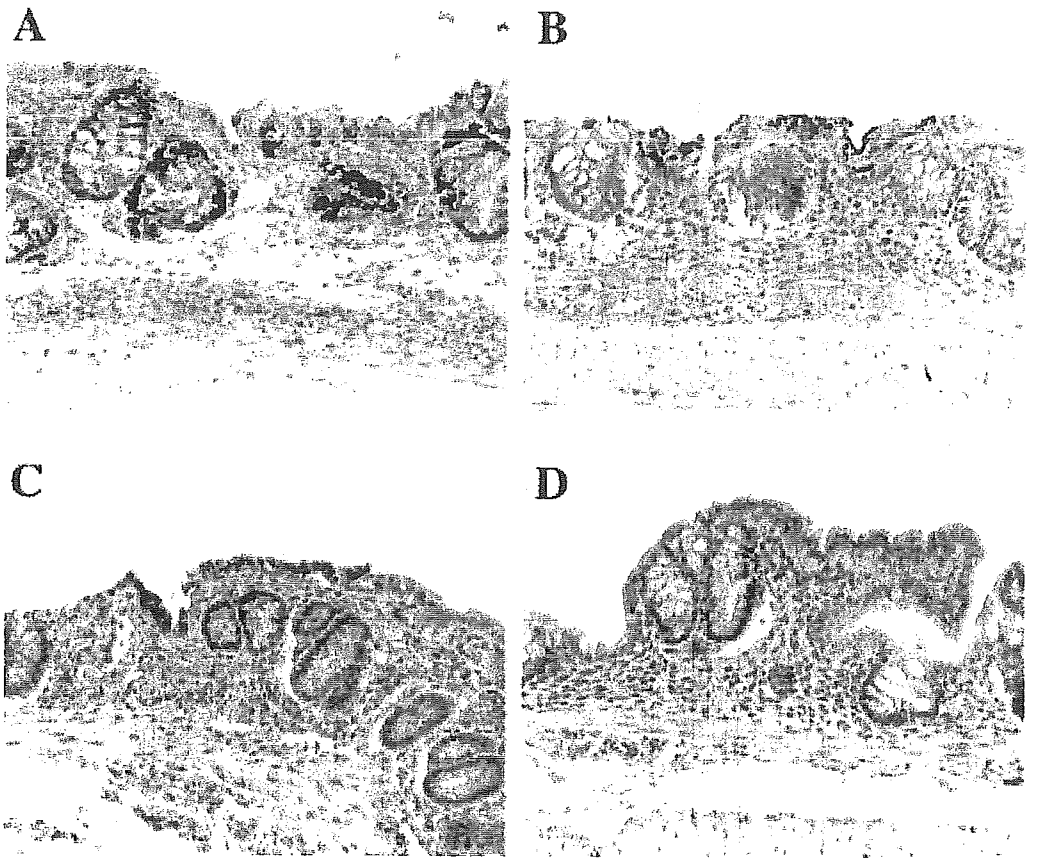

Fig. 6. Nitrotyrosine immunohistochemistry of the colon from four strains of mice given 1% DSS. (**A**) Balb/c; (**B**) C3H/HeN; (**C**) C57BL/6N; and (**D**) DBA/2N.Original magnification, (A–D), 20×.

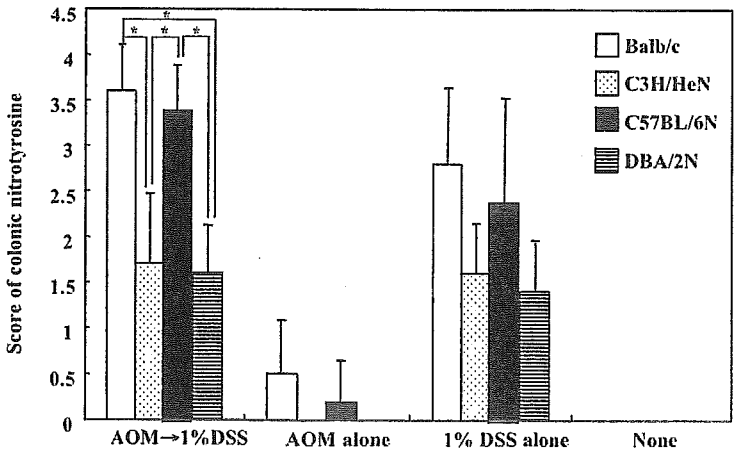

Fig. 7. Score for nitrotyrosine immunohistochemistry. Values are the mean ± SD. White column, Balb/c; white column with dots, C3H/HeN; black columns, C57BL/6N; striped columns, DBA/2N. $^{*}P < 0.001$.

(27,28). In the current study, the sensitivities of the four strains to DSS were somewhat dissimilar to those of previous studies (27,28). The inflammation score of colonic mucosa revealed a severe and moderate inflammation to be present in the C3H/HeN and Balb/c mice treated with both AOM and DSS, respectively, while C57BL/6N and DBA/2N mice had only a relatively weak inflammation. In the case of the receptivity of C57BL mice to lipopolysaccharide (LPS), C57BL/10ScCr mice were resistant to LPS, whereas C57BL/10ScSn mice responded to LPS (37). Similarly, C3H/HeJ and C3H/HeN are LPS-responder and LPS-non-responder mice, respectively (38,39). As a result, the discrepancy in the response of DSS in mice might be due to differences in the substrains. In the current study, the highest incidence of colonic tumors was

found in Balb/c. C57BL/6N had the second highest incidence among the strains tested. On the other hand, C3H/HeN and DBA/2N had only a few benign colonic tumors (adenomas). The shortening of colon length in the mice that received DSS is one of the biological markers of severity of colonic inflammation (8–10,32,35). When comparing the colon length in mice treated with AOM and DSS with that in untreated mice, the order of the shortening rate of the colon length of mice was Balb/c (7%) > C57BL/6N (4%) > DBA/2N (3%) > C3H/HeN (−6%). These results suggest that the different susceptibilities of the inbred mouse strains to AOM/DSS-induced colon carcinogenesis might correlate with different sensitivities to AOM or DSS, with only slight contradictions among the substrains.

AOM is widely used as a colonic carcinogen to investigate the pathogenesis and modification of colon carcinogenesis in rodents (11–13). AOM requires metabolic activation to exert its carcinogenic action. Cytochrome P450 (CYP) is known to play a prominent role in the modulation of the xenobiotic metabolism, including chemical carcinogens. CYP 2E1 is one of the important factors for converting AOM to methylazoxymethanol, which can produce DNA adduct formation and also produce the initiation event (40,41). Although we did not investigate the activity of CYP 2E1, it may be possible that the expression and/or content of CYP 2E1 differ among the strains examined. This may be indicated by the findings that the relative liver weight of Balb/c, which had the highest susceptibility of AOM/DSS-induced colon carcinogenesis, was higher than that of other strains of mice in the current study (data not shown).

The influence of nitrosation stress caused by DSS is also an important factor for AOM/DSS-induced mouse colon carcinogenesis, since a powerful tumor-promoting activity of DSS has been observed in this model (8,32,35,42). We found a close association between the score of nitrotyrosine and the occurrence of tumors in the current study. Nitrotyrosine-immunohistochemical scores of each strain of mice in the 'AOM → DSS' and 'DSS alone' groups were much greater than those of the 'AOM alone' and 'untreated' groups. The scores of the 'AOM → DSS' group were relatively higher than those of the 'DSS alone' group in all strains of mice and the order was Balb/c > C57BL/6N > C3H/HeN > DBA/2N in these two groups. Such inflammation could influence tumorigenesis, although the inflammation score did not completely correspond with the frequency of colonic tumors in the current study. Indeed, the score of inflammation in the mice receiving both AOM and DSS was higher than that of the mice administered DSS alone. An investigation of additional factors is needed to precisely elucidate the strain differences in the susceptibility to colon carcinogenesis. Recently Greten *et al.* (43) reported interesting findings, namely that a specific inactivation of the IκB kinase (IKK)/NF-κB pathway can attenuate the formation of inflammation-associated colon tumors in *villin-Cre/Ikkβ*$^{F/\Delta}$ mice. They also suggested that IKKβ might be involved in inflammation-related carcinogenesis.

In conclusion, we herein demonstrated the differences in the genetic susceptibility to AOM/DSS-induced colon tumorigenesis among four inbred strains (Balb/c, C3H/HeN, C57BL/6N and DBA/2N) of mice and found the Balb/c mice to be the most sensitive. Our findings suggest that the genetic background thus plays an important role in the cancer risk in colitis-related colon tumorigenesis. In addition, strain differences in the susceptibility of colon carcinogenesis induced by AOM and DSS might be influenced by the response to nitrosation stress due to inflammation as determined by the genetic background.

Acknowledgements

This work was supported in part by a Grant-in-Aid for Cancer Research, for the Third-Term Comprehensive 10-Year Strategy for Cancer Control from the Ministry of Health, Labour and Welfare of Japan; the Grants-in-Aid (No. 15·2052) for Scientific Research from the Ministry of Education, Culture, Sports, Science and Technology of Japan; and a grant (H2004-6) for Project Research from the High-Technology Center of Kanazawa Medical University.

Conflict of Interest Statement: None declared.

References

1. Jemal,A., Tiwari,R.C., Murray,T., Ghafoor,A., Samuels,A., Ward,E., Feuer,E.J. and Thun,M.J. (2004) Cancer statistics, 2004. *CA. Cancer J. Clin.*, **54**, 8–29.
2. Itzkowitz,S.H. and Yio,X. (2004) Inflammation and cancer IV. Colorectal cancer in inflammatory bowel disease: the role of inflammation. *Am. J. Physiol. Gastrointest. Liver Physiol.*, **287**, G7–G17.
3. Brostrom,O., Lofberg,R., Nordenvall,B., Ost,A. and Hellers,G. (1987) The risk of colorectal cancer in ulcerative colitis. An epidemiologic study. *Scand. J. Gastroenterol.*, **22**, 1193–1199.
4. Ekbom,A., Helmick,C., Zack,M. and Adami,H.O. (1990) Ulcerative colitis and colorectal cancer. A population-based study. *N. Engl. J. Med.*, **323**, 1228–1233.
5. Greenstein,A.J. (2000) Cancer in inflammatory bowel disease. *Mt Sinai J. Med.*, **67**, 227–240.
6. Ambs,S., Merriam.W.G., Bennett,W.P., Felley-Bosco,E., Ogunfusika,M.O., Oser,S.M., Klein,S., Shields,P.G., Billiar,T.R. and Harris,C.C. (1998) Frequent nitric oxide synthase-2 expression in human colon adenomas: implication for tumor angiogenesis and colon cancer progression. *Cancer Res.*, **58**, 334–341.
7. Macarthur,M., Hold,G.L. and El-Omar,E.M. (2004) Inflammation and Cancer II. Role of chronic inflammation and *cytokine* gene polymorphisms in the pathogenesis of gastrointestinal malignancy. *Am. J. Physiol. Gastrointest. Liver Physiol.*, **286**, G515–G520.
8. Tanaka,T., Kohno,H., Suzuki,R., Yamada,Y., Sugie,S. and Mori,H. (2003) A novel inflammation-related mouse colon carcinogenesis model induced by azoxymethane and dextran sodium sulfate. *Cancer Sci.*, **94**, 965–973.
9. Tanaka,T., Suzuki,R., Kohno,H., Sugie,S., Takahashi,M. and Wakabayashi,K. (2005) Colonic adenocarcinomas rapidly induced by the combined treatment with 2-amino-1-methyl-6-phenylimidazo [4,5-*b*]pyridine and dextran sodium sulfate in male ICR mice possess b-catenin gene mutations and increases immunoreactivity for b-catenin, cyclooxygenase-2, and inducible nitric oxide synthase. *Carcinogenesis*, **26**, 229–238.
10. Kohno,H., Suzuki,R., Sugie,S. and Tanaka,T. (2005) b-Catenin mutations in a mouse model of inflammation-related colon carcinogenesis induced by 1,2-dimethylhydrazine and dextran sodium sulfate. *Cancer Sci.*, **96**, 69–76.
11. Hata,K., Yamada,Y., Kuno,T., Hirose,Y., Hara,A., Qiang,S.H. and Mori,H. (2004) Tumor formation is correlated with expression of b-catenin-accumulated crypts in azoxymethane-induced colon carcinogenesis in mice. *Cancer Sci.*, **95**, 316–320.
12. Yang,K., Lamprecht,S.A., Liu,Y., Shinozaki,H., Fan,K., Leung,D., Newmark,H., Steele,V.E., Kelloff,G.J. and Lipkin,M. (2000) Chemoprevention studies of the flavonoids quercetin and rutin in normal and azoxymethane-treated mouse colon. *Carcinogenesis*, **21**, 1655–1660.
13. Takahashi,M., Nakatsugi,S., Sugimura,T. and Wakabayashi,K. (2000) Frequent mutations of the b-*catenin* gene in mouse colon tumors induced by azoxymethane. *Carcinogenesis*, **21**, 1117–1120.
14. Okayasu,I., Hatakeyama,S., Yamada,M., Ohkusa,T., Inagaki,Y. and Nakaya,R. (1990) A novel method in the induction of reliable experimental acute and chronic ulcerative colitis in mice. *Gastroenterology*, **98**, 694–702.
15. Kitajima,S., Morimoto,M. and Sagara,E. (2002) A model for dextran sodium sulfate (DSS)-induced mouse colitis: bacterial degradation of DSS

does not occur after incubation with mouse cecal contents. *Exp. Anim.*, **51**, 203–206.
16. Hirono,I., Kuhara,K., Hosaka,S., Tomizawa,S. and Golberg,L. (1981) Induction of intestinal tumors in rats by dextran sulfate sodium. *J. Natl Cancer Inst.*, **66**, 579–583.
17. Tham,D.M., Whitin,J.C. and Cohen,H.J. (2002) Increased expression of extracellular glutathione peroxidase in mice with dextran sodium sulfate-induced experimental colitis. *Pediatr. Res.*, **51**, 641–646.
18. Cooper,H.S., Murthy,S., Kido,K., Yoshitake,H. and Flanigan,A. (2000) Dysplasia and cancer in the dextran sulfate sodium mouse colitis model. Relevance to colitis-associated neoplasia in the human: a study of histopathology, b-catenin and p53 expression and the role of inflammation. *Carcinogenesis*, **21**, 757–768.
19. Deschner,E.E., Hakissian,M. and Long,F.C. (1989) Genetic factors controlling inheritance of susceptibility to 1,2-dimethylhydrazine. *J. Cancer Res. Clin. Oncol.*, **115**, 335–339.
20. Festing,M.F. (1995) Use of a multistrain assay could improve the NTP carcinogenesis bioassay. *Environ. Health Perspect.*, **103**, 44–52.
21. Fujita,H., Nagano,K., Ochiai,M., Ushijima,T., Sugimura,T., Nagao,M. and Matsushima,T. (1999) Difference in target organs in carcinogenesis with a heterocyclic amine, 2-amino-3,4-dimethylimidazo [4,5-*f*]quinoline, in different strains of mice. *Jpn. J. Cancer Res.*, **90**, 1203–1206.
22. Gressani,K.M., Leone-Kabler,S., O'Sullivan,M.G., Case,L.D., Malkinson,A.M. and Miller,M.S. (1999) Strain-dependent lung tumor formation in mice transplacentally exposed to 3-methylcholanthrene and post-natally exposed to butylated hydroxytoluene. *Carcinogenesis*, **20**, 2159–2165.
23. Papanikolaou,A., Wang,Q.-S., Papanikolaou,D., Whiteley,H.E. and Rosenberg,D. (2000) Sequential and morphological analyses of aberrant crypt foci formation in mice of differing susceptibility to azoxymethane-induced colon carcinogenesis. *Carcinogenesis*, **21**, 1567–1572.
24. Tsuda,H., Naito,A., Kim,C., Fukamachi,K., Nomoto,H. and Moore,M.A. (2003) Carcinogenesis and its modification by environmental endocrine disruptors: in vivo experimental and epidemiological findings. *Jpn. J. Clin. Oncol.*, **33**, 259–270.
25. Wang,Q.S., Walsh,A., Goldsby,J.S., Papanikolaou,A., Bolt,A.B. and Rosenberg,D.W. (1999) Preliminary analysis of azoxymethane-induced colon tumorigenesis in mouse aggregation chimeras. *Carcinogenesis*, **20**, 691–697.
26. Nambiar,P.R., Girnun,G., Lillo,N.A., Guda,K., Whiteley,H.E. and Rosenberg,D.W. (2003) Preliminary analysis of azoxymethane induced colon tumors in inbred mice commonly used as transgenic/knockout progenitors. *Int. J. Oncol.*, **22**, 145–150.
27. Mahler,M., Bristol,I.J., Leiter,E.H., Workman,A.E., Birkenmeier,E.H., Elson,C.O. and Sundberg,J.P. (1998) Differential susceptibility of inbred mouse strains to dextran sulfate sodium-induced colitis. *Am. J. Physiol.*, **274**, G544–G551.
28. Stevceva,L., Pavli,P., Buffinton,G., Wozniak,A. and Doe,W.F. (1999) Dextran sodium sulphate-induced colitis activity varies with mouse strain but develops in lipopolysaccharide-unresponsive mice. *J. Gastroenterol. Hepatol.*, **14**, 54–60.
29. Pereira,M.A., Tao,L.H., Wang,W., Gunning,W.T. and Lubet,R. (2005) Chemoprevention: mouse colon and lung tumor bioassay and modulation of DNA methylation as a biomarker. *Exp. Lung Res.*, **31**, 145–163.
30. Singer,I.I., Kawka,D.W., Scott,S., Weidner,J.R., Mumford,R.A., Riehl,T.E. and Stenson,W.F. (1996) Expression of inducible nitric oxide synthase and nitrotyrosine in colonic epithelium in inflammatory bowel disease. *Gastroenterology*, **111**, 871–885.
31. Murata,M. and Kawanishi,S. (2004) Oxidative DNA damage induced by nitrotyrosine, a biomarker of inflammation. *Biochem. Biophys. Res. Commun.*, **316**, 123–128.
32. Suzuki,R., Kohno,H., Sugie,S. and Tanaka,T. (2005) Dose-dependent promoting effect of dextran sodium sulfate on mouse colon carcinogenesis initiated with azoxymethane. *Histol. Histopathol.*, **20**, 483–492.
33. Cooper,H.S., Murthy,S.N., Shah,R.S. and Sedergran,D.J. (1993) Clinicopathologic study of dextran sulfate sodium experimental murine colitis. *Lab. Invest.*, **69**, 238–249.
34. Krutovskikh, V.A. and Turusov, V.S. (1994) Tumours of the intestines. In Turusov,V.S. and Mohr,V. (eds) *Pathology of Tumors in Laboratory Animals*. Vol. 2-Tumours of the Mouse. IARC Scientific Publications No. 111, Lyon, pp. 195–221.
35. Suzuki,R., Kohno,H., Sugie,S. and Tanaka,T. (2004) Sequential observations on the occurrence of preneoplastic and neoplastic lesions in mouse colon treated with azoxymethane and dextran sodium sulfate. *Cancer Sci.*, **95**, 721–727.
36. Zingarelli,B., Szabo,C. and Salzman,A.L. (1999) Reduced oxidative and nitrosative damage in murine experimental colitis in the absence of inducible nitric oxide synthase. *Gut.*, **45**, 199–209.
37. Muller,I., Freudenberg,M., Kropf,P., Kiderlen,A.F. and Galanos,C. (1997) Leishmania major infection in C57BL/10 mice differing at the *Lps* locus: a new non-healing phenotype. *Med. Microbiol. Immunol. (Berl.)*, **186**, 75–81.
38. Watson,J., Riblet,R. and Taylor,B.A. (1977) The response of recombinant inbred strains of mice to bacterial lipopolysaccharides. *J. Immunol.*, **118**, 2088–2093.
39. Watson,J. and Riblet,R. (1974) Genetic control of responses to bacterial lipopolysaccharides in mice. I. Evidence for a single gene that influences mitogenic and immunogenic respones to lipopolysaccharides. *J. Exp. Med.*, **140**, 1147–1161.
40. Sohn,O.S., Ishizaki,H., Yang,C.S. and Fiala,E.S. (1991) Metabolism of azoxymethane, methylazoxymethanol and *N*-nitrosodimethylamine by cytochrome P450 IIE1. *Carcinogenesis*, **12**, 127–131.
41. Sohn,O.S., Fiala,E.S., Requeijo,S.P., Weisburger,J.H. and Gonzalez,F.J. (2001) Differential effects of CYP2E1 status on the metabolic activation of the colon carcinogens azoxymethane and methylazoxymethanol. *Cancer Res.*, **61**, 8435–8440.
42. Tanaka,T., Kohno,H., Suzuki,R., Hata,K., Sugie,S., Niho,N., Sakano,K., Takahashi,M. and Wakabayashi,K. (2005) Dextran sodium sulfate strongly promotes colorectal carcinogenesis in *Apc*$^{-/+}$ mice: Inflammatory stimuli by dextran sodium sulfate results in development of multiple colonic neoplasms. *Int. J. Cancer*, in press.
43. Greten,F.R., Eckmann,L., Greten,T.F., Park,J.M., Li,Z.W., Egan,L.J., Kagnoff,M.F. and Karin,M. (2004) IKKb links inflammation and tumorigenesis in a mouse model of colitis-associated cancer. *Cell*, **118**, 285–296.

Received June 8, 2005; revised July 24, 2005; accepted July 28, 2005

Int. J. Cancer: **118,** 2232–2236 (2006)

Predominant T helper type 2-inflammatory responses promote murine colon cancers

Emi Osawa[1,2], Atsushi Nakajima[2], Toshio Fujisawa[2], Yuki I. Kawamura[1,3], Noriko Toyama-Sorimachi[1], Hitoshi Nakagama[4] and Taeko Dohi[1]*

[1]*Department of Gastroenterology, Research Institute, International Medical Center of Japan, Tokyo, Japan*
[2]*Gastroenterology Division, Yokohama City University School of Medicine, Yokohama, Japan*
[3]*GS platZ Co. Ltd., Tokyo, Japan*
[4]*Biochemistry Division, National Cancer Center Research Institute, Tokyo, Japan*

Colon cancer is one of the most serious complications of inflammatory bowel diseases, especially ulcerative colitis (UC). Previous studies have shown that characteristic immunological event during inflammation in UC is the expression of T helper-type 2 (Th2) cell-derived cytokines. In this study, we investigated the influence of a predominant Th2-type cytokine response in colitis on carcinogen-induced colon tumors. Wild type (WT), interferon gamma (IFN-γ) gene deficient (−/−) [Th2 dominant] or interleukin (IL)-4$^{-/-}$ [Th1-dominant] mice of BALB/c background were used in this study. To compare tumor formation, mice were given the carcinogen azoxymethane (AOM) and intrarectal administration of trinitrobenzene sulfonic acid (TNBS), to induce colitis. Thirty-three weeks after initial treatment, the total colon was examined. When IFN-γ$^{-/-}$ mice were treated with AOM and TNBS, significantly higher number of tumors were seen (8.4 ± 1.7) than in WT (3.3 ± 2.9) or IL-4$^{-/-}$ (3.1 ± 3.4) mice, which received identical treatments. A separate set of experiment, using less doses of AOM and TNBS also showed the higher frequency of tumor formation in IFN-γ$^{-/-}$ mice than in IL-4$^{-/-}$ mice. Histologically, the tumors were well- or moderately-differentiated adenocarcinomas. No invasion into the submucosal or serosal layers of the intestine was seen. In immunohistological staining, some tumors in IFN-γ$^{-/-}$ mice showed distinct nuclear expression of β-catenin, in contrast to the strong membrane staining seen in tumors of IL-4$^{-/-}$ mice. In conclusion, colonic inflammation associated with Th2-donimant cytokine responses enhanced the formation of malignant neoplasms.

Key words: colitis; cancer; interferon-γ; interleukin-4; carcinogenesis

Colorectal cancer is one of the most serious complications in inflammatory bowel diseases (IBD), including ulcerative colitis (UC) and Crohn's disease (CD).[1] Of note, patients with longstanding, extensive UC have a high cancer risk, ~16.5% at 30 years, after initial diagnosis.[2,3] It has long been noted that cancer arises from regions of chronic inflammation, and the inflammatory cells and cytokines of the immune system found in tumors are more likely to contribute to tumor growth and progression.[4] In animal models, colitis induced by dextran sulfate sodium (DSS) are associated with dysplasia and cancer.[5–7] Recent studies on liver cancer[8] and colon cancer[9] models suggested that transcription factor NF-κB, which is a key player of inflammatory responses, does not affect initiation, but acts in tumor promotion. Thus, inflammation may significantly affect the process of cancer in UC. In fact, cancers in UC have several distinct features from colorectal cancers in non-IBD patients.[10] First, tumors in UC are often multiple, which is to be expected from precancerous dysplastic changes found in UC mucosa. Second, cancer in UC is often flat and infiltrating. Third, there is a higher incidence of high-grade, mucinous carcinomas than seen in non-IBD cancer. At a molecular level, p53 gene mutations or p53 protein overexpression, which is a late event in the development of sporadic colorectal carcinoma, have been commonly reported as early events in the dysplasia–carcinoma sequences in UC-associated carcinomas.[11–14] These results provide evidence that UC-associated cancer may develop along a pathway that is different from that of sporadic colorectal cancer.

Although pathogenesis of IBD is unknown, fluctuating but constant inflammatory responses at the local site is the major pathological finding. Past studies have shown that local immunological events during chronic inflammation in UC and CD are different. The presence of activated Th1 cells in the intestine is the characteristic of CD, with high expression of interferon gamma (IFN-γ) and tumor necrosis factor alpha (TNF-α).[15,16] On the other hand, elevated expression of T helper-type 2 (Th2) cell-derived cytokines is often seen in UC.[17,18] By use of various murine models, we and others have shown that such distinct cytokine responses actually involved in the unique pathological changes in CD and UC. For example, we noted distinct pathological differences in the hapten-induced colitis in Th1 *versus* Th2-dominant mice.[19,20] In Th2 dominant mice, fibrosis and diffuse atrophic changes in epithelial cells were seen, while acute ulcers were the major lesions of colitis in Th1 dominant mice. Other groups have reported that administration of the sensitizing agent, oxazolone, induced colitis with diffuse epithelial damage. In this model, a Th2 type cytokine, interleukin (IL)-13 was the major effector cytokine.[21,22] Further, transfer of Th2-dominant T cells to T cell-deficient recipient mice resulted in ileal villus atrophy and goblet cell metaplasia,[23] while transfer of Th1 dominant T cells induced erosive gastritis with enhanced surface epithelial cell apoptosis.[24] These results suggest that a predominance of either Th1- or Th2-type cytokines in inflammatory responses has a major influence on the pathology and tissue remodeling in the chronic inflammation, and eventually affects controlling epithelial cell differentiation, as well as their turnover. Thus, differential upregulation of inflammatory cytokines in UC may directly contribute to malignant progression. However, data on the participation of a predominance of Th1 or Th2 cytokines in mucosal immunity in colonic carcinogenesis is limited.

The possible factors which lead to dysplasia and malignant transformation in UC need to be more thoroughly investigated. In this study, we used models of Th1- or Th2-dominant colitis model together with azoxymethane (AOM)-induced carcinogenesis and sequential and morphological analysis, paying particular attention to the tissue tropism of carcinogenesis. Our findings show that a Th2 cytokine dominant colitis increases the frequency and changes in pathological features of colonic neoplasms.

Abbreviations: AOM, azoxymethane; DSS, dextran sulfate sodium; GI, gastrointestinal; H&E, hematoxylin and eosin; IFN, interferon; IL, interleukin; TNBS, trinitrobenzene sulfonic acid; TNF, tumor necrosis factor.

Grant sponsors: Ministry of Health, Labor, and Welfare; International Health Cooperation Research; Ministry of Education, Culture, Sports, Science, and Technology; Japan Health Sciences Foundation and Organization; Organization for Pharmaceutical Safety and Research.

***Correspondence to:** Department of Gastroenterology, Research Institute, International Medical Center of Japan, 1-21-1 Toyama, Shinjuku-ku, Tokyo 162-8655, Japan. Fax: +81-3-3202-7364.
E-mail: dohi@ri.imcj.go.jp

Received 10 August 2005; Accepted 29 September 2005
DOI 10.1002/ijc.21639
Published online 5 December 2005 in Wiley InterScience (www.interscience.wiley.com).

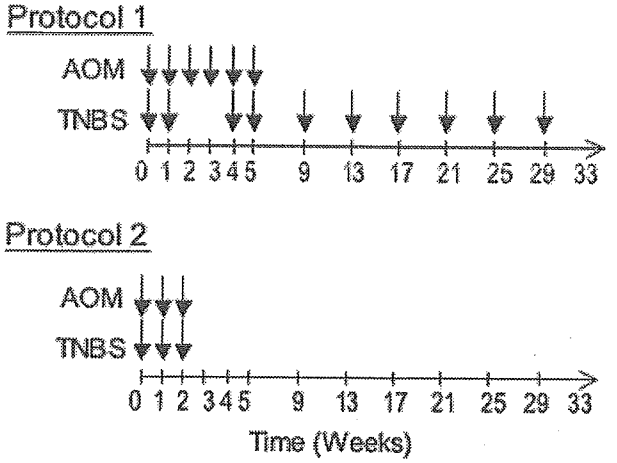

FIGURE 1 – Experimental design used in this study.

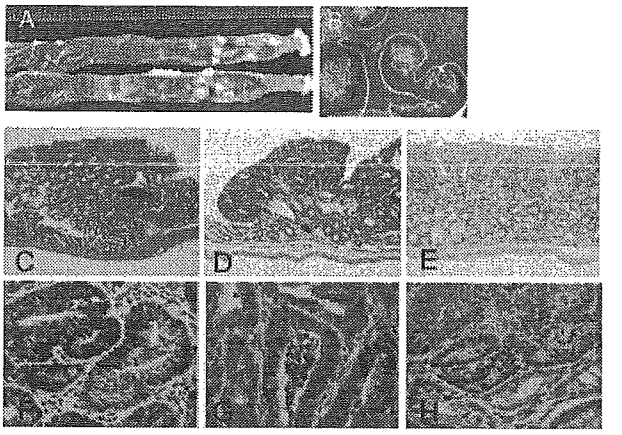

FIGURE 2 – Pathological features of colonic tumors. (*a*) Macroscopic appearance of typical tumors. Colons from IFN-$\gamma^{-/-}$ mice treated with AOM plus TNBS are shown. (*b*) Zoom stereomicroscopic appearance of tumors in panel A after staining with methylene blue. Polypoid cancer seen in WT (*c*) and IL-$4^{-/-}$ (*d*) mice treated with AOM plus TNBS, stained by H&E. (*e*) Flat-elevated cancer seen in IFN-$\gamma^{-/-}$ mice (H&E staining). Immunostaining for β-catenin of well-differentiated adenocarcinomas from WT (*f*) and IL-$4^{-/-}$ (*g*) mice showing a cell membrane pattern and moderately differentiated adenocarcinoma from IFN-$\gamma^{-/-}$ mice (*f*) showing a nuclear pattern.

Material and methods

Mice

Wild type (WT), IFN-γ gene knockout (IFN-$\gamma^{-/-}$), IL-4 gene disrupted (IL-$4^{-/-}$) mice, all on the BALB/c background were originally obtained from Jackson Laboratory (Bar Harbor, ME). The colony was maintained under pathogen-free conditions in the Immunocompromized Mouse Facility of the Research Institute, International Medical Center of Japan (IMCJ). All experiments were performed according to the Institutional Guidelines for the Care and Use of Laboratory Animals in Research and according to the approval of the local ethics committee in the IMCJ.

Induction of colitis and colon tumors

Treatment of mice was initiated when mice were 8 weeks of age. Trinitrobenzene sulfonic acid (TNBS) colitis was induced, as described previously.[19,20] A 2% solution of TNBS (Research Organics, Cleveland, OH) in PBS:ethanol (1:1 by volume) was administered intrarectally to mice, anesthetized with ketamine (Sankyo Co. Ltd., Tokyo, Japan) and xylazine (Sigma, St. Louis, MO). A dose of TNBS of 36 μg/g of body weight was given. The colon carcinogen AOM was purchased from Sigma, and a dose of 10 μg/g of body weight in saline was injected intraperitoneally. TNBS and AOM were given, as indicated (Fig. 1). In some experimental groups, treatment with either TNBS or AOM was performed. In protocol 1, six doses of AOM or 4 doses of TNBS were given during the first 5 weeks, and then TNBS was given every 4 weeks on 6 occasions, to mimic recurrence of inflammation. In protocol 2, three doses of TNBS and AOM were given together in the first 2 weeks, and colonic tissues were examined after 33 weeks. To examine the spontaneous development of tumors, some cytokine knockout mice were kept untreated, until they were 40 weeks of age.

Macroscopic and histological examination

Colonic tissues were opened longitudinally, fixed in 10% formalin overnight at 4°C, washed in PBS, stained with 2% methylene blue for contrast, and then the numbers of macroscopically visible tumors were assessed. Some specimens were examined with a zoom stereomicroscope. Tumors were removed along with the surrounding normal colonic tissues and embedded in paraffin blocks; then, 4-μm sections were prepared and stained with hematoxylin and eosin (H&E). For immunohistochemical analysis, 3-μm-thick paraffin sections were deparaffinated in xylene, rehydrated and heated at 95°C in 10 mM citrated buffer (pH 6.0) for 10 min. After treatment with 3% H_2O_2, followed by 0.25% goat serum in PBS for blocking, sections were incubated with monoclonal antibodies to p53 (DO-1, 1:200) or β-catenin (1:800, both from BD Transduction Laboratories, CA) overnight at 4°C. Mouse IgG was used as a negative control. Bound antibody was detected using Vectastain ABD-kit (Vector Laboratories, Burlingame, CA) according to vendor's protocol, and deaminobenzidine was used as substrate for peroxidase.

Statistics

The results were compared by the Mann–Whitney test or χ^2 test, using the Statview II statistical program (Abacus Concepts, Berkeley, CA) adapted for the Macintosh computer.

Results

Effects of inflammation and cytokine deficiency on the formation of colon tumors

In our study, polypoid or sessile elevated lesions were macroscopically visible in the middle to distal colon, and these were enumerated (Figs. 2*a* and 2*b*). The results of protocol 1 are summarized in Table I. When WT mice were treated with only AOM in protocol 1, 3.3 tumors/mouse were seen after 33 weeks. In IFN-$\gamma^{-/-}$ mice, the incidence of tumors induced with AOM was not significantly different from that of WT mice. IL-$4^{-/-}$ mice, treated with AOM only, did not develop tumors, except for 1 mouse with a single tumor, although aberrant crypt foci (ACF) were frequently seen by following zoom stereomicroscopy. Induction of TNBS colitis, in addition to AOM treatment, did not change the numbers of tumors in WT mice. In contrast, induction of colitis induced enhanced formation of tumors in both IFN-$\gamma^{-/-}$ and IL-$4^{-/-}$ mice. Of note, the number of tumors in IFN-$\gamma^{-/-}$ mouse reached to 8 tumors/mouse, which was significantly higher when compared with those in IL-$4^{-/-}$ or WT mice. The incidence of tumor bearing mice was 100% in the IFN-$\gamma^{-/-}$ group. There were no significant differences in the size of the tumors, which developed in each experimental group. In protocol 1, most of the deaths occurred mostly in the first 8 weeks. The exceptions were that some IL-$4^{-/-}$ mice treated with TNBS died in later period, coinciding with our previous report that IL-$4^{-/-}$ mice are more susceptible to TNBS colitis.[19] Further, we did not see any tumors in the mice which died before 33 weeks, including IL-$4^{-/-}$ mice.

TABLE I – NUMBER OF TUMORS IN CYTOKINE DEFICIENT MICE (PROTOCOL 1)

Mice	Treatment	No. of mice survived/total	Incidence of tumor	No. of tumors/mouse	Size of tumors (mm^3)	Total number of tumors
WT	AOM	7/12 (58)[1]	5/7 (71)	3.3 ± 2.9	2.2 ± 1.3	23
WT	AOM + TNBS	10/17 (59)	6/10 (60)	2.0 ± 2.5	2.9 ± 1.3	20
WT	TNBS	5/5 (100)	0/5 (0)	0 ± 0		0
IFN-$\gamma^{-/-}$	AOM	7/16 (43)	2/7 (28)	1.4 ± 2.3	2.7 ± 1.9	10
IFN-$\gamma^{-/-}$	AOM + TNBS	7/11 (64)	7/7 (100)[2]	8.3 ± 1.8[3]	2.8 ± 1.8	58
IFN-$\gamma^{-/-}$	TNBS	8/10 (80)	0/8 (0)	0 ± 0		0
IFN-$\gamma^{-/-}$	Untreated	8/8 (100)	0/8 (0)	0 ± 0		0
IL-$4^{-/-}$	AOM	15/17 (88)	1/15 (7)	0.1 ± 0.3[4]	1.6	1
IL-$4^{-/-}$	AOM+TNBS	7/11 (64)	5/7 (71)[5]	3.1 ± 3.4	1.7 ± 1.2	22
IL-$4^{-/-}$	TNBS	2/7 (29)	0/2 (0)	0 ± 0		0
IL-$4^{-/-}$	Untreated	4/4 (100)	0/4 (0)	0 ± 0		0

[1]Values in parentheses indicate percentages.–[2]Difference from IFN-$\gamma^{-/-}$ or IL-$4^{-/-}$ mice treated AOM was statistically significant ($p<0.02$).–[3]Differences from all other experimental groups were statistically significant ($p < 0.02$).–[4]Differences from WT mice with AOM or AOM+TNBS were statistically significant ($p<0.02$).–[5]Difference from IL-$4^{-/-}$ mice treated AOM was statistically significant ($p < 0.02$).

TABLE II – NUMBERS OF TUMORS IN CYTOKINE DEFICIENT MICE (PROTOCOL 2)

Mice	Treatment	No. of mice survived/total	Incidence of tumor formation	No. of tumors/mouse	Total number of tumors
IFN-$\gamma^{-/-}$	AOM + TNBS	19/24 (79)[1]	10/19[2] (53)	0.8 ± 0.9[2]	15
IL-$4^{-/-}$	AOM + TNBS	12/24 (50)	0/12 (0)	0	0

[1]Values in parentheses indicate percentages.–[2]Differences from IL-$4^{-/-}$ mice were statistically significant ($p < 0.02$).

It indicated that mortality was not associated with cancer, but more with susceptibility to TNBS colitis or toxicity of AOM in each mouse strain.

Next, to conform the difference between IL-$4^{-/-}$ and IFN-$\gamma^{-/-}$ mice treated with both AOM and TNBS, we have chosen protocol 2 (Fig. 1), reducing the dose of AOM and TNBS. A change in the dose of AOM improved the survival of IFN-$\gamma^{-/-}$ mice; however, this dose change did not affect the survival of IL-$4^{-/-}$ mice, probably because of their higher sensitivity to TNBS colitis than IFN-$\gamma^{-/-}$ mice (Table II). In this protocol, death occurred within the first 3 weeks, and no tumor-caused death was observed in both groups. Although the numbers of tumor/mouse decreased in this protocol, we saw similar differences between the IFN-$\gamma^{-/-}$ and IL-$4^{-/-}$ mice groups (Table II). No visible tumors were seen in IL-$4^{-/-}$ mice. In contrast, 10 of 19 IFN-$\gamma^{-/-}$ mice formed more than 1 tumor in the colon.

Microscopic findings

Tumors formed in protocol 1 were subjected to microscopic examination. The majority of these were polypoid lesions (Figs. 2*c* and 2*d*), and some of them were flat, elevated lesions (Fig. 2*e*). Tumors histologically examined were all diagnosed as well-differentiated or moderately differentiated adenocarcinoma. There was also colonic dysplasia involving 1–2 crypts, in mouse groups that had treatment with AOM. In each groups of mice, there were no differences in the severity of cell infiltration into tumors. In IFN-$\gamma^{-/-}$ mice with TNBS colitis, deformity of crypts was the most evident, as previously reported[20]; however, there were no clear relations to tumor location. In WT mice, the ratio of moderately differentiated adenocarcinoma from mice treated with both AOM and TNBS tended to be higher than those treated only with AOM, in which well-differentiated adenocarcinoma was the major type (Fig. 3). The majority of tumors from IFN-$\gamma^{-/-}$ mice were moderately differentiated adenocarcinomas in both AOM or AOM plus TNBS treated groups (Fig. 3). In protocol 2, fourteen out of 15 tumors from IFN-$\gamma^{-/-}$ mice treated with AOM plus TNBS were also diagnosed as moderately differentiated adenocarcinomas. One tumor was a well-differentiated adenocarcinoma.

Immunohistochemistry

Immunostaining for p53 and β-catenin was performed. Staining with anti-p53 monoclonal antibody was generally weak, and obviously enhanced nuclear staining was seen in only 2 tumors in IFN-$\gamma^{-/-}$ mice treated with AOM plus TNBS, 2 from IL-$4^{-/-}$ mice

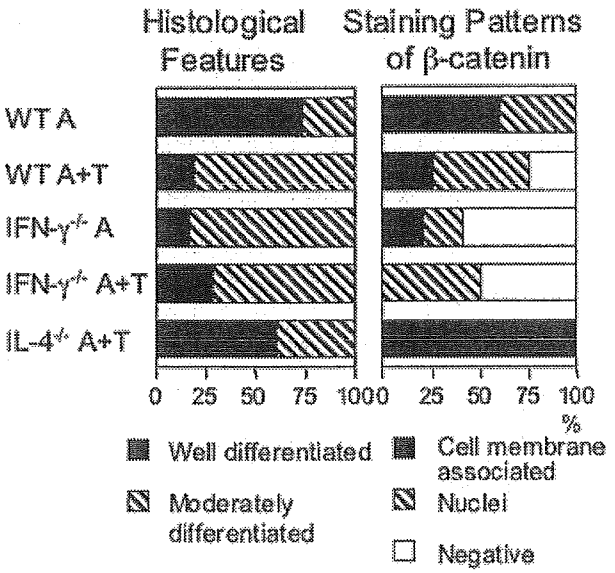

FIGURE 3 – Percentage of histological diagnosis and β-catenin staining pattern of colon tumors. Tumors (6–10) from each mouse group in protocol 1 were evaluated for their histological grading and expression of β-catenin. A, treated with AOM; T, treated with TNBS.

treated with AOM plus TNBS and 2 tumors from WT mice treated with AOM (data not shown). In contrast, a differential staining pattern with β-catenin was seen. Well-differentiated adenocarcinomas in WT and IL-$4^{-/-}$ mice showed typical staining of cell membrane, which was much stronger than that in normal epithelial cells (Figs. 2*f* and 2*g*). In contrast, nuclear staining was frequently observed in tumors from IFN-$\gamma^{-/-}$ mice treated with AOM plus TNBS (Fig. 2*h*). All tumors from IL-$4^{-/-}$ mice showed a cell membrane pattern, including the one from mice treated with only AOM. There was no tumor with a membrane-staining pattern from IFN-$\gamma^{-/-}$ mice treated with AOM plus TNBS (Fig. 3). Thus, nuclear and membrane localization of β-catenin was the characteristics of moderately differentiated adenocarcinomas in IFN-$\gamma^{-/-}$ mice and well-differentiated adenocarcinoma in IL-$4^{-/-}$ mice, respectively (Fig. 3).

Discussion

In the present study comparing WT, IFN-$\gamma^{-/-}$ and IL-$4^{-/-}$ mice, several new findings in colitis-related colon cancer were revealed. First, in the absence of IFN-γ, induction of TNBS colitis and AOM strongly enhanced tumor formation in the colon. Importantly, colitis also affected the histological degree of differentiation, and frequently induced nuclear translocation of β-catenin.

Although the precise mechanism of enhancement of tumor formation is not yet clear, one possibility is that a defect of tumor immunosurveillance occurs in IFN-$\gamma^{-/-}$ mice. Previous studies showed that IFN-$\gamma^{-/-}$ mice develop chemical carcinogen methylcholanthrene-induced sarcoma,[25] spontaneous lymphomas and lung adenocarcinomas[26] more frequently than do WT mice. In our studies, there were no significant differences in the frequency of tumor formation between WT and IFN-$\gamma^{-/-}$ mice, when inflammation was not induced. In contrast, in the presence of colitis, the number of tumors in IFN-$\gamma^{-/-}$ mice was markedly increased, while tumor frequency in WT mice was not increased. This result in WT mice is distinct from studies reporting the development of AOM-induced tumors within a short term in WT mice when DSS colitis was induced,[27,28] although there has been no report testing IFN-$\gamma^{-/-}$ mice. In DSS colitis, diffuse loss of epithelium is the primary pathological finding, which might increase the chance of carcinogenesis and promotion during vigorous epithelial cell regeneration. On the other hand, since TNBS colitis is characterized by a focal ulcer and a strong hapten (trinitrophenyl residue)-specific immune response of T and B cells, IFN-γ produced as a part of adoptive immunity in the inflammation seems to be important for protection from the colonic tumor. In other words, IFN-γ production may not be required for tumor surveillance in non-inflamed, steady state colons of BALB/c mice. A significant incidence of lung carcinoma, but no report of colon carcinoma during the life span of more than 600 days in BALB/c IFN-$\gamma^{-/-}$ mice, also supports this notion.[26] The importance of IFN-γ in tumor surveillance produced by T cells as a part of adoptive immunity was also shown in the previous study that $RAG2^{-/-}$ x $STAT1^{-/-}$ double knockout mice showed increased susceptibly to methylcholanthrene-induced carcinogenesis, but did not display a significantly greater tumor incidence, when compared with mice that lacked either RAG2 or STAT1 genes.[25] Thus, it is feasible that the colonic mucosa of UC, which fails to induce prevailing upregulation of IFN-γ but produces Th2-type cytokines, can frequently develop colonic carcinoma. On the other hand, our results also showed that addition of TNBS colitis to AOM increased the incidence of tumor in IL-$4^{-/-}$ mice, although the number was much less than in IFN-$\gamma^{-/-}$ mice. This result suggested that aberrant Th1-dominant inflammatory responses might also increase the tumor risk, although it was not comparable to that in Th2 dominant condition.

Since there is an interaction between Th1 and Th2 cytokines that they suppress the effect of each other, the presence of an excess amount of Th2 cytokines in IFN-$\gamma^{-/-}$ would have a significant effect. We have previously analyzed the cytokine production by colonic $CD4^+$ cells in WT, IL-$4^{-/-}$ and IFN-$\gamma^{-/-}$ mice in naïve colon, as well as in acute (day 1) and chronic (day 10) phase of TNBS colitis. Colonic $CD4^+$ T cells from IFN-$\gamma^{-/-}$ mice produced very large amounts of IL-4 and IL-5. In contrast, secretion of IFN-γ by colonic $CD4^+$ T cells from IL-$4^{-/-}$ mice was higher than in colonic $CD4^+$ T cells from WT mice.[19,20] In protocol 1 of current study, the number of tumors in IL-$4^{-/-}$ mice was much lower than those of WT or IFN-$\gamma^{-/-}$ mice. In protocol 2, none of the IL-$4^{-/-}$ mice developed tumors, in contrast to the 53% incidence in IFN-$\gamma^{-/-}$ mice. These results suggest that IL-4 may have a direct effect on promoting tumor formation. In fact, many malignant tumors express the IL-4 receptor, which is able to bind to both IL-4 and IL-13 and also the high affinity decoy receptor of IL-13, IL-13 receptor α2.[29] However, the function of IL-4 and IL-13 in tumor cells, especially in colonic cancer is not yet clear, and the output effect via these receptors still remains to be investigated. Early studies showed that IL-4 and IL-13 had antitumor activity in mice by growth inhibition[30] through IL-4 receptor.[31] However, subversion of host antitumor defenses has also been demonstrated for IL-13. Recent studies using tumor cell lines demonstrated that STAT6, IL-4 and IL-13 were capable of inhibiting tumor rejection.[32–34] Thus, Th2 type cytokines appear to antagonize tumor immunosurveillance.

In our study, IL-$4^{-/-}$ mice and IFN-$\gamma^{-/-}$ mice showed distinct expression patterns for β-catenin, cell membrane and nuclear staining in IL-$4^{-/-}$ and IFN-$\gamma^{-/-}$ mice, respectively, while WT mice had tumors of both patterns. This again suggests that Th2-cytokine predominance directly influences the mutation of DNA in epithelial cells. Indeed, exogenous IL-4 and IL-13 decreased the levels of membrane staining of β-catenin in keratinocytes, without changes of total protein levels of β-catenin, while IFN-γ enhanced membrane staining.[35] In our model, gene mutation induced by AOM might facilitate nuclear translocation of β-catenin, which had localized in cytoplasm, but not in cell membrane by the action of IL-4 and IL-13, secreted as inflammatory responses of IFN-$\gamma^{-/-}$ mice. Thus, we propose that enhancement of tumor formation in IFN-$\gamma^{-/-}$ mice is due both to a lack of immunosurveillance by IFN-γ and promotion of carcinogenesis by excess Th2 type cytokines. In this context, epithelial cells in the process of tissue repair in the inflamed colon are susceptible to the absence of IFN-γ and the presence of excess amount of IL-4 and IL-13.

In summary, our results show that a predominance of Th2 type cytokines in the inflamed colon, which mimics mucosal immunity in UC, promotes aberrant β-catenin expression and tumor formation. This model will be useful to further clarify the mechanism of colitic-cancer and for our search for targets or new agents for prevention of colon cancer.

References

1. Eaden JA, Abrams KR, Mayberry JF. The risk of colorectal cancer in ulcerative colitis: a meta-analysis. Gut 2001;48:526–35.
2. Allison M, Dhillon A, Lewis W, Pounder R, eds. Inflammatory bowel disease. London: Mosby, 1998. 111–19.
3. Gyde SN, Prior P, Allan RN, Stevens A, Jewell DP, Truelove SC, Lofberg R, Brostrom O, Hellers G. Colorectal cancer in ulcerative colitis: a cohort study of primary referrals from three centres. Gut 1988;29:206–17.
4. Balkwill F, Mantovani A. Inflammation and cancer: back to Virchow? Lancet 2001;357:539–45.
5. Cooper HS, Murthy S, Kido K, Yoshitake H, Flanigan A. Dysplasia and cancer in the dextran sulfate sodium mouse colitis model. Relevance to colitis-associated neoplasia in the human: a study of histopathology, B-catenin and p53 expression and the role of inflammation. Carcinogenesis 2000;21:757–68.
6. Hirono I, Kuhara K, Hosaka S, Tomizawa S, Golberg L. Induction of intestinal tumors in rats by dextran sulfate sodium. J Natl Cancer Inst 1981;66:579–83.
7. Yamada M, Ohkusa T, Okayasu I. Occurrence of dysplasia and adenocarcinoma after experimental chronic ulcerative colitis in hamsters induced by dextran sulphate sodium. Gut 1992;33:1521–7.
8. Pikarsky E, Porat RM, Stein I, Abramovitch R, Amit S, Kasem S, Gutkovich-Pyest E, Urieli-Shoval S, Galun E, Ben-Neriah Y. NF-kappaB functions as a tumour promoter in inflammation-associated cancer. Nature 2004;431:461–6.
9. Greten FR, Eckmann L, Greten TF, Park JM, Li ZW, Egan LJ, Kagnoff MF, Karin M. IKKbeta links inflammation and tumorigenesis in a mouse model of colitis-associated cancer. Cell 2004;118: 285–96.
10. Day DW, Jass JR, Price AB, Shepherd NA, Sloan JM, Talbot IC, Warren BF, Williams GT, eds. Morson and Dawson's gastrointestinal pathology. Oxford: Blackwell, 2003. 472–539.
11. Lashner BA, Shapiro BD, Husain A, Goldblum JR. Evaluation of the usefulness of testing for p53 mutations in colorectal cancer surveillance for ulcerative colitis. Am J Gastroenterol 1999;94:456–62.
12. Ilyas M, Talbot IC. p53 expression in ulcerative colitis: a longitudinal study. Gut 1995;37:802–4.
13. Yin J, Harpaz N, Tong Y, Huang Y, Laurin J, Greenwald BD, Hontanosas M, Newkirk C, Meltzer SJ. p53 point mutations in dysplastic

and cancerous ulcerative colitis lesions. Gastroenterology 1993;104: 1633–9.
14. Brentnall TA, Crispin DA, Rabinovitch PS, Haggitt RC, Rubin CE, Stevens AC, Burmer GC. Mutations in the p53 gene: an early marker of neoplastic progression in ulcerative colitis. Gastroenterology 1994; 107:369–78.
15. Parronchi P, Romagnani P, Annunziato F, Sampognaro S, Becchio A, Giannarini L, Maggi E, Pupilli C, Tonelli F, Romagnani S. Type 1 T-helper cell predominance and interleukin-12 expression in the gut of patients with Crohn's disease. Am J Pathol 1997;150:823–32.
16. Kakazu T, Hara J, Matsumoto T, Nakamura S, Oshitani N, Arakawa T, Kitano A, Nakatani K, Kinjo F, Kuroki T. Type 1 T-helper cell predominance in granulomas of Crohn's disease. Am J Gastroenterol 1999;94:2149–55.
17. Fuss IJ, Neurath M, Boirivant M, Klein JS, de la Motte C, Strong SA, Fiocchi C, Strober W. Disparate $CD4^+$ lamina propria (LP) lymphokine secretion profiles in inflammatory bowel disease. Crohn's disease LP cells manifest increased secretion of IFN-gamma, whereas ulcerative colitis LP cells manifest increased secretion of IL-5. J Immunol 1996;157:1261–70.
18. Inoue S, Matsumoto T, Iida M, Mizuno M, Kuroki F, Hoshika K, Shimizu M. Characterization of cytokine expression in the rectal mucosa of ulcerative colitis: correlation with disease activity. Am J Gastroenterol 1999;94:2441–6.
19. Dohi T, Fujihashi K, Kiyono H, Elson CO, McGhee JR. Mice deficient in Th1- and Th2-type cytokines develop distinct forms of hapten-induced colitis. Gastroenterology 2000;119:724–33.
20. Dohi T, Fujihashi K, Rennert PD, Iwatani K, Kiyono H, McGhee JR. Hapten-induced colitis is associated with colonic patch hypertrophy and T helper 2-type responses. J Exp Med 1999;189:1169–80.
21. Heller F, Fuss IJ, Nieuwenhuis EE, Blumberg RS, Strober W. Oxazolone colitis, a Th2 colitis model resembling ulcerative colitis, is mediated by IL-13-producing NK-T cells. Immunity 2002;17:629–38.
22. Boirivant M, Fuss IJ, Chu A, Strober W. Oxazolone colitis: a murine model of T helper cell type 2 colitis treatable with antibodies to interleukin 4. J Exp Med 1998;188:1929–39.
23. Dohi T, Fujihashi K, Koga T, Shirai Y, Kawamura YI, Ejima C, Kato R, Saitoh K, McGhee JR. T helper type-2 cells induce ileal villus atrophy, goblet cell metaplasia and wasting disease in T cell-deficient mice. Gastroenterology 2003;124:672–82.
24. Dohi T, Fujihashi K, Koga T, Etani Y, Yoshino N, Kawamura YI, McGhee JR. $CD4^+CD45RB^{Hi}$ inteleukin-4 defective T cells elicit antral gastritis and duodenitis. Am J Pathol 2004;165:1257–68.
25. Shankaran V, Ikeda H, Bruce AT, White JM, Swanson PE, Old LJ, Schreiber RD. IFNgamma and lymphocytes prevent primary tumour development and shape tumour immunogenicity. Nature 2001;410: 1107–11.
26. Street SE, Trapani JA, MacGregor D, Smyth MJ. Suppression of lymphoma and epithelial malignancies effected by interferon gamma. J Exp Med 2002;196:129–34.
27. Tanaka T, Kohno H, Suzuki R, Yamada Y, Sugie S, Mori H. A novel inflammation-related mouse colon carcinogenesis model induced by azoxymethane and dextran sodium sulfate. Cancer Sci 2003;94:965–73.
28. Becker C, Fantini MC, Schramm C, Lehr HA, Wirtz S, Nikolaev A, Burg J, Strand S, Kiesslich R, Huber S, Ito H, Nishimoto N, et al. TGF-beta suppresses tumor progression in colon cancer by inhibition of IL-6 trans-signaling. Immunity 2004;21:491–501.
29. Wynn TA. IL-13 effector functions. Annu Rev Immunol 2003;21: 425–56.
30. Puri R. Structure and function of interleukin 4 and its receptors. In: Kurzrock R, Talpaz M, eds. Cytokines: interleukins and their receptors. Norwell: Kluwer, 1995.143–85.
31. Renard N, Duvert V, Banchereau J, Saeland S. Interleukin-13 inhibits the proliferation of normal and leukemic human. Blood 1994;84: 2253–60.
32. Ostrand-Rosenberg S, Grusby MJ, Clements VK. Cutting edge: STAT6-deficient mice have enhanced tumor immunity to primary and metastatic mammary carcinoma. J Immunol 2000;165:6015–19.
33. Kacha AK, Fallarino F, Markiewicz MA, Gajewski TF. Cutting edge: spontaneous rejection of poorly immunogenic P1.HTR tumors by Stat6-deficient mice. J Immunol 2000;165:6024–8.
34. Terabe M, Matsui S, Noben-Trauth N, Chen H, Watson C, Donaldson DD, Carbone DP, Paul WE, Berzofsky JA. NKT cell-mediated repression of tumor immunosurveillance by IL-13 and the IL-4R-STAT6 pathway. Nat Immunol 2000;1:515–20.
35. Fujii-Maeda S, Kajiwara K, Ikizawa K, Shinazawa M, Yu B, Koga T, Furue M, Yanagihara Y. Reciprocal regulation of thymus and activation-regulated chemokine/macrophage-derived chemokine production by interleukin (IL)-4/IL-13 and interferon-gamma in HaCaT keratinocytes is mediated by alternations in E-cadherin distribution. J Invest Dermatol 2004;122:20–8.

Available online at www.sciencedirect.com
SCIENCE DIRECT®
ELSEVIER
Mutation Research xxx (2006) xxx–xxx
Fundamental and Molecular Mechanisms of Mutagenesis
www.elsevier.com/locate/molmut
Community address: www.elsevier.com/locate/mutres

Molecular mechanisms for maintenance of G-rich short tandem repeats capable of adopting G4 DNA structures

Hitoshi Nakagama*, Kumiko Higuchi, Etsuko Tanaka, Naoto Tsuchiya, Katsuhiko Nakashima, Masato Katahira, Hirokazu Fukuda

Biochemistry Division, National Cancer Center Research Institute, 5-1-1 Tsukiji, Chuo-ku, Tokyo 104-0045, Japan

Abstract

Mammalian genomes contain several types of repetitive sequences. Some of these sequences are implicated in various specific cellular events, including meiotic recombination, chromosomal breaks and transcriptional regulation, and also in several human disorders. In this review, we document the formation of DNA secondary structures by the G-rich repetitive sequences that have been found in several minisatellites, telomeres and in various triplet repeats, and report their effects on in vitro DNA synthesis. d(GGCAG) repeats in the mouse minisatellite Pc-1 were demonstrated to form an intra-molecular folded-back quadruplex structure (also called a G4′ structure) by NMR and CD spectrum analyses. d(TTAGGG) telomere repeats and d(CGG) triplet repeats were also shown to form G4′ and other unspecified higher order structures, respectively. In vitro DNA synthesis was substantially arrested within the repeats, and this could be responsible for the preferential mutability of the G-rich repetitive sequences. Electrophoretic mobility shift assays using NIH3T3 cell extracts revealed heterogeneous nuclear ribonucleoprotein (hnRNP) A1 and A3, which were tightly and specifically bound to d(GGCAG) and d(TTAGGG) repeats with K_d values in the order of nM. HnRNP A1 unfolded the G4′ structure formed in the $d(GGCAG)_n$ and $d(TTAGGG)_n$ repeat regions, and also resolved the higher order structure formed by d(CGG) triplet repeats. Furthermore, DNA synthesis arrest at the secondary structures of d(GGCAG) repeats, telomeres and d(CGG) triplet repeats was efficiently repressed by the addition of hnRNP A1. High expression of hnRNPs may contribute to the maintenance of G-rich repetitive sequences, including telomere repeats, and may also participate in ensuring the stability of the genome in cells with enhanced proliferation. Transcriptional regulation of genes, such as *c-myc* and *insulin*, by G4 sequences found in the promoter regions could be an intriguing field of research and help further elucidate the biological functions of the hnRNP family of proteins in human diseases.

Keywords: Molecular mechanism; G4 DNA structure; G-rich repetitive sequence; hnRNPs

1. Introduction

Mammalian genomes are known to contain various types of repetitive sequences, including microsatellites, triplet repeats, minisatellites, and telomeres [1]. LINE, SINE and LTR sequences are also frequently found in the genome of vertebrates [2]. Although there is some variation in the size definition for repeat families, microsatellite repeats are generally composed of short repetitive units of less than 6 nucleotides [1]. It is estimated that more than 100,000 microsatellite loci occur in the mammalian genome. Microsatellites are typically less than 100 base pairs (bp) in total length [3]. Although triplet repeats are also categorized as members of the microsatellite family, some triplet repeat loci can

* Corresponding author. Tel.: +81 3 3547 5239; fax: +81 3 3542 2530.
E-mail address: hnakagam@gan2.res.ncc.go.jp (H. Nakagama).

0027-5107/$ – see front matter © 2006 Elsevier B.V. All rights reserved.
doi:10.1016/j.mrfmmm.2006.01.014